Applied Soil Ecology 219 (2026) 106808

Contents lists available at ScienceDirect

Applied Soil Ecology

journal homepage: www.elsevier.com/locate/apsoil

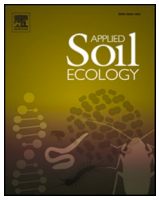

Research paper

Microbial-mediated shifts regulate the trade-off between soil organic carbon content and stability after cropland afforestation in Eastern China

Jie Liu [a], Lin Yang [a,*], Jie Wang [a], Lei Zhang [c], Yongqi Qian [d], Ren Wei [a], Wenkai Cui [a], Chenghu Zhou [a,b]

[a] School of Geography and Ocean Science, Nanjing University, Nanjing, 210023, China
[b] State Key Laboratory of Resources and Environmental Information System, Institute of Geographic Sciences and Natural Resources Research, Chinese Academy of Sciences, Beijing, 100101, China
[c] Climate and Ecosystem Science Division, Lawrence Berkeley National Laboratory, Berkeley, CA, 94720, USA
[d] State Key Laboratory of Efficient Utilization of Arable Land in China, Institute of Agricultural Resources and Regional Planning, Chinese Academy of Agricultural Sciences, Beijing, 100081, China

ARTICLE INFO

Keywords:
Soil organic carbon
Particulate organic carbon
Mineral-associated organic carbon
Microbial-derived carbon
Croplands
Planted forests

ABSTRACT

Cropland soil organic carbon (SOC) is a vital component of the global carbon cycle. At the same time, the expansion of adjacent planted forests, driven by their ecological benefits, further shapes regional carbon dynamics. This offers a pivotal research opportunity to investigate divergences in SOC and its fractions, as well as carbon formation and stabilization mechanisms in croplands and planted forests converted from croplands. Elucidating divergent influencing mechanisms of SOC and its fractions between croplands and planted forests is critical to deciphering different land-use impacts on carbon storage and optimizing land-use-specific carbon sequestration management under global warming. We collected 39 paired cropland-planted forest soil samples in a major grain-producing region of Eastern China, and used piecewise structural equation modeling and random forest modeling to quantify and compare the effects of physical carbon parameters, microbial-derived carbon (MDC), and biotic-abiotic drivers on SOC and its fractions between croplands and adjacent planted forests. Croplands exhibited significantly higher SOC, particulate organic carbon (POC), and mineral-associated organic carbon (MAOC) contents than planted forests, exceeding forest levels by 34%, 68%, and 25%, respectively. Compared to planted forests, croplands had a higher POC proportion but a lower MAOC proportion. Furthermore, the dominant drivers of SOC, POC, and MAOC shifted from biotic factors in croplands to abiotic factors in planted forests. Dissolved organic carbon (DOC) exhibited a stronger positive contribution to SOC accumulation in croplands than in planted forests. Fungal necromass carbon (FNC) contributed more to SOC, POC, and MAOC than bacterial necromass carbon (BNC) in croplands, but the opposite was true in planted forests. Collectively, planted forests exhibited lower but more stable SOC compared to croplands, demonstrating greater sensitivity to abiotic drivers and stronger MAOC dominance (constituting 78.85% of total SOC). Conversely, cropland SOC was primarily regulated by biotic drivers and MDC inputs. Therefore, land-use-specific management is essential to maximize the complementary carbon sequestration potentials of croplands and planted forests, thereby enhancing global SOC accumulation and stabilization.

Abbreviations: SOC, soil organic carbon; POC, particulate organic carbon; MAOC, mineral-associated organic carbon; POM, particulate organic matter; MAOM, mineral-associated organic matter; MDC, microbial-derived carbon; DOC, dissolved organic carbon; BNC, bacterial necromass carbon; FNC, fungal necromass carbon; MNC, microbial necromass carbon; NAC, microbial necromass accumulation coefficient; $MAOC_{max}$, the theoretical maximum of MAOC; CSD, MAOC saturation degree; MBC, microbial biomass carbon; PCP, soil physical carbon parameters; AMF, arbuscular mycorrhizal fungi; EcMF, ectomycorrhizal fungi; SWC, soil water content; SBD, soil bulk density; EC, electrical conductivity; TN, total nitrogen; NH_4^+-N, ammonium nitrogen; NO_3^--N, nitrate nitrogen; NO_2^--N, nitrite nitrogen; TP, total phosphorus; AP, available phosphorus; TK, total potassium; AK, available potassium; MAT, mean annual temperature; MAP, mean annual precipitation; SWE, snow water equivalent; TWI, topographic wetness index; SPI, stream power index; FVC, fractional vegetation cover; NPP, net primary production; SP, soil properties; MKT, microbial key taxa (i.e., top10 abundant taxa); MN, microbial network topology properties, containing microbial community structure properties; MD, microbial community taxonomic and functional diversity; Network.PC1, first principal component extracted using sub-network topology properties; Network.PC2, second principal component extracted using sub-network topology properties.

* Corresponding author at: School of Geography and Ocean Science, Nanjing University, Nanjing, 210023, China.
E-mail address: yanglin@nju.edu.cn (L. Yang).

https://doi.org/10.1016/j.apsoil.2026.106808
Received 14 October 2025; Received in revised form 11 December 2025; Accepted 12 January 2026

1. Introduction

Soil organic carbon (SOC) represents the largest terrestrial carbon pool, playing critical roles in regulating the global carbon cycle and mitigating climate change through carbon sequestration practices (Batjes, 1996; Crowther et al., 2019). Among terrestrial ecosystems, cropland soils constitute a pivotal carbon reservoir whose dynamics directly influence atmospheric CO_2 concentrations (Derrien et al., 2023). In agricultural landscapes, particularly those dominated by intensive cropping systems, planted forests are commonly established along field margins or irrigation canals. Despite their relatively small spatial extent compared to adjacent croplands, these planted forest patches hold significant ecological value within agroecosystems. Planted forests have become one focus of current research as they have emerged as a globally widespread significant climate mitigation initiative, recognized for their carbon sequestration potential (Cheng et al., 2024). Crucially, the distinct vegetation types and management practices between croplands and adjacent planted forests are likely to drive fundamental differences in SOC formation and stabilization mechanisms, leading to variations in SOC and its fraction contents (Wang et al., 2025b). However, while existing studies have quantified contrasts in SOC and its fractions between croplands and natural forests, the differences in the content, formation, and stabilization pathways of SOC and its fractions between croplands and adjacent planted forests are still unclear.

Divergent hydro-nutrient regimes and associated carbon formation and stabilization pathways drive contrasting contents of particulate organic carbon (POC) and mineral-associated organic carbon (MAOC), alongside their differential contributions to SOC pools, between cropland and planted forests (Derrien et al., 2023). POC originates primarily from the fragmentation and translocation of litter residues and lacks mineral association, whereas MAOC derives mainly from microbial necromass complexed with mineral surfaces (Derrien et al., 2023; Li et al., 2024). Distinguishing POC and MAOC provides essential mechanistic insights into SOC cycling across land-use types (von Lützow et al., 2007; Angst et al., 2023). MAOC persists for centuries due to stabilization via strong organo-mineral bonding and physical protection within microaggregates. In contrast, POC, composed largely of partially decomposed plant fragments, is inherently more labile and susceptible to microbial decomposition (von Lützow et al., 2007; Angst et al., 2023). Consequently, unless physically occluded, POC exhibits a relatively short soil residence time (Lavallee et al., 2020; Angst et al., 2023; Zhou et al., 2024). Notably, soils with lower SOC content tend to store a greater proportion of carbon as MAOC rather than POC (Derrien et al., 2023). As such, POC or MAOC predominance varies characteristically across land-use types (Derrien et al., 2023; Liu et al., 2025b).

Given its physicochemical protection mechanisms, MAOC is widely recognized as a stable, persistent SOC fraction (Lavallee et al., 2020; Heckman et al., 2022). Consequently, a higher MAOC/SOC ratio serves as a robust indicator of prolonged SOC turnover times at the ecosystem scale (Sokol et al., 2022). Physical occlusion within aggregates also protects POC by reducing microbial accessibility (Zhou et al., 2024). When designing carbon-focused management strategies to enhance POC and MAOC levels, the MAOC saturation degree (CSD) should be assessed (Angst et al., 2023; Soinne et al., 2024). As MAOC approaches its saturation limit, strategies targeting MAOC formation for SOC storage may become ineffective or even promote priming losses (Cotrufo et al., 2022; Li et al., 2024). The contrasting dynamics of POC and MAOC necessitate their separation within a conceptual framework to evaluate carbon sequestration potential accurately (Cotrufo et al., 2019). Therefore, investigating POC and MAOC divergence in cropland-adjacent planted forests provides a spatially explicit framework for optimizing carbon management. Aligning strategies with the inherent complexity of SOC pools is key to leveraging soils as sustainable carbon sinks, constituting an essential step toward achieving climate mitigation targets (Angst et al., 2023).

Dissolved organic carbon (DOC) acts as a critical precursor regulating SOC dynamics, particularly the formation pathways of POC and MAOC. This regulation occurs through a sequential microbial pathway: DOC assimilation into microbial biomass carbon (MBC), followed by transformation into microbial necromass carbon (MNC). Crucially, microbial necromass forms the dominant carbon source for MAOC, stabilized primarily through this DOC-microbial pathway (Sokol and Bradford, 2019). Despite constituting less than 2% of SOC, DOC represents one of the most biogeochemically active and mobile carbon pools in terrestrial systems (von Lützow et al., 2007). As the most labile SOC fraction, DOC exhibits rapid turnover, ranging from hours to months (Deng et al., 2021). It serves as the primary substrate for microbial metabolism, critically influences soil acid-base equilibria, and modulates nutrient bioavailability via chelation and transport (Marschner and Bredow, 2002). Molecular-level studies indicate that ambient temperature and soil water content (SWC) distinctly control microbial transformation of DOC into POC or MAOC (Niu et al., 2024). Furthermore, soil microbial diversity and network complexity significantly influence MBC and MNC production, thereby governing SOC storage (Wang et al., 2021; Wang et al., 2023). Notably, microbial community composition often exerts a stronger control on SOC accumulation than clay mineralogy, with microbial-derived carbon (MDC) accumulation being most pronounced in soils exhibiting higher fungal abundance and efficient microbial biomass production (Kallenbach et al., 2016). A critical yet poorly understood aspect of soil carbon cycling is the mechanistic disconnection between microbial activity and the formation of stable carbon fractions. To bridge this gap, we introduce DOC and MNC as key carbon parameters that link microbial processes to carbon stabilization. This establishes a continuous pathway from microbial assimilation of DOC to the transformation of MBC into MNC and its subsequent contribution to POC and MAOC formation. Using this framework, we quantify the proportional contributions of these pathways to SOC accumulation in croplands and adjacent planted forests.

The aforementioned processes are co-regulated by biotic and abiotic drivers governing carbon formation and stabilization in croplands and planted forests (Lehmann and Kleber, 2015; Wang et al., 2025b). Abiotic drivers encompass soil properties, climate, topography, and vegetation characteristics (Luo et al., 2017; Li et al., 2025b), with temperature, precipitation, pH, nitrogen, and phosphorus significantly influencing SOC, POC, and MAOC dynamics (Gao et al., 2024; Zhou et al., 2024). Higher soil silt content and SWC further promote MAOC accumulation (Niu et al., 2024). Biotic drivers—including the diversity, composition, structure, and network complexity of bacterial, fungal, archaeal, and mycorrhizal communities—exert pronounced control over SOC and its fractions (Sokol et al., 2022; Wang et al., 2023). Mycorrhizal association type represents a key biotic factor, influencing SOC dynamics through variations in tissue degradability and organic matter decomposition capacity (Cotrufo et al., 2019). Critically, the relative effects and interactions of these diverse abiotic and biotic factors on SOC, POC, MAOC, and related carbon parameters remain systematically quantified in croplands and adjacent planted forests.

Eastern China, such as the Yangtze River Delta—characterized by intensive agriculture, urban expansion, and widespread afforestation—serves as an ideal area to investigate SOC and its fraction divergence between croplands and adjacent planted forests. We propose the following research hypotheses: (1) SOC in croplands exhibits higher content than in adjacent planted forests; (2) SOC in adjacent planted forests exhibits higher stability than in croplands; (3) the contribution of DOC to SOC formation and stabilization may differ between croplands and adjacent planted forests due to differences in hydro-nutrient regimes; (4) the influencing mechanisms on SOC and its fractions in croplands and adjacent planted forests may differ due to habitat-specific soil microbe-plant-environment interactions. Based on the above hypotheses, the objectives of the study are: (1) to compare the differences in soil carbon parameters and soil properties between croplands and adjacent planted forests; (2) to quantify and compare the relative

importance of abiotic factors (e.g., climatic factors, terrain factors, vegetation factors, soil properties), biotic factors (e.g., soil microbial composition, taxonomic and functional diversity, structure, network complexity), MDC (e.g., MNC, MBC), or soil physical carbon parameters (PCP) (e.g., CSD, DOC, POC, MAOC) for SOC and its fraction regulation between croplands and adjacent planted forests; (3) to elucidate and quantify the direct and indirect contributions of interactions among distinct soil carbon parameters within the pathway through which DOC is transformed into SOC and its fractions via the microbial carbon pump. This study aims to provide targeted soil carbon management measures for sustainable development and combating climate change, directly contributing to global climate mitigation goals like the '4 per 1000 - soils for food security and climate' initiative.

2. Materials and methods

2.1. Study sites and soil sampling

The study area is situated in Jiangsu Province, Eastern China (Fig. 1), within the warm-temperate to subtropical summer monsoon climate zone, spanning semi-humid and humid regimes. Most of the region experiences a subtropical humid climate. The terrain is predominantly low-lying plains, with scattered low hills in the north and southwest. Sampled croplands primarily comprised rice paddies and rice-wheat rotation systems. Adjacent planted forests, established primarily on former cropland 10–20 years prior, experience lower anthropogenic disturbance than cropland soils. The planted forests in our sampling area primarily consisted of *Populus* spp., *Betula* spp., *Cunninghamia lanceolata*, and *Zelkova serrata*. The dominant tree species in these stands is the *Populus* spp.

Soil was sampled at the depths of 0–20 cm in early October 2023 using a stainless-steel hand auger (inner diameter of 5 cm). The determination of sampling sites was mainly based on the Latin Hypercube sampling method (Minasny and McBratney, 2006). We used a five-point sampling method for sampling (Mao et al., 2020). The distance between each pair of cropland and forest soils in the sampling point shall not exceed 1 km. We collected a total of 78 samples (Fig. 1a) scattered across typical cropland and adjacent planted forest soils (Fig. 1b) in the study area (116°49′ E–121°39′ E, 30°78′ N–34°65′ N). The sampling sites experienced a mean annual temperature (MAT) between 14.28 and 16.65 °C (Fig. S1a) and a mean annual precipitation (MAP) from 730.91 to 1181.66 mm (Fig. S1b).

After collection, soil samples were transported to the laboratory within 6 h in insulated boxes with ice packs. Upon arrival, subsamples (10 g) of cropland and forest soils were placed in sterile 50 mL centrifuge tubes and immediately stored at −80 °C for DNA extraction and subsequent high-throughput sequencing. The remaining soil samples were stored at 4 °C for the analysis of soil properties and carbon parameters.

The detailed methodologies for determining soil physicochemical properties [e.g., SWC, soil bulk density (SBD), pH, electrical conductivity (EC), total nitrogen (TN), ammonium nitrogen (NH_4^+-N), nitrate nitrogen (NO_3^--N), nitrite nitrogen (NO_2^--N), total phosphorus (TP), available phosphorus (AP), total potassium (TK), and available potassium (AK)] and metallic elements (Ca, Mg, Mn, Cr, Cd, and Cu), alongside the sources and collection procedures for climate [MAT, MAP, and snow water equivalent (SWE)], terrain [elevation, topographic wetness index (TWI), stream power index (SPI), and slope], and vegetation [fractional vegetation cover (FVC) and net primary production (NPP)] data, are described in the Supplementary Material.

2.2. Soil carbon parameters analysis and calculation

Prior to analysis, air-dried soil was sieved through a 100-mesh (0.15 mm) sieve. SOC was then determined by the $K_2Cr_2O_7$-H_2SO_4 oxidation method (Mebius, 1960) and titrated with $FeSO_4$ solution. DOC was extracted with 0.5 M K_2SO_4 and analyzed by a TOC analyzer (TOC-L; Shimadzu, Tokyo, Japan). MBC was measured employing the chloroform fumigation-extraction method (Wu et al., 1990).

We separated soil fractions using a wet-sieving technique based on Marriott and Wander (2006). In this procedure, 10 g of air-dried soil (passed through a 2 mm sieve) was subjected to dispersion with 150 mL of 5‰ sodium hexametaphosphate on a shaker operating at 200 rpm for 18 h. The dispersed mixture was then passed through a 53 μm sieve under a stream of deionized water, yielding two particle-size fractions: particulate organic matter (POM, >53 μm) and mineral-associated organic matter (MAOM, <53 μm). All fractions were oven-dried at 50 °C, weighed, and finally ground to pass a 100-mesh (0.15 mm) sieve before their carbon content was determined by the same method applied for SOC.

The contents of POC and MAOC in soil (in g/kg) were calculated using the following formulas:

$$POC = C_{POM} \times W_{POM}/W_{soil} \quad (1)$$

where C_{POM} denotes the carbon content of the POM fraction (g/kg), W_{POM} is the weight of the POM fraction (g), and W_{soil} represents the initial mass of the soil sample (g).

$$MAOC = C_{MAOM} \times W_{MAOM}/W_{soil} \quad (2)$$

where C_{MAOM} denotes the carbon content of the MAOM fraction (g/kg), W_{MAOM} is the weight of the MAOM fraction (g), and W_{soil} represents the initial mass of the soil sample (g).

The theoretical maximum of MAOC ($MAOC_{max}$, g/kg) was calculated according to Six et al. (2002):

$$MAOC_{max} = 0.26 \times P_{MAOM} + 5.5 \quad (3)$$

where P_{MAOM} denotes the proportion of 50 μm MAOM (%).

CSD (%) was estimated as follows:

$$CSD = MAOC/MAOC_{max} \times 100 \quad (4)$$

2.3. Amino sugars analysis and calculation

Amino sugars were extracted and quantified to determine MNC following the method of Zhang and Amelung (1996). Subsequently, the extracts were analyzed using an Agilent 6890A gas chromatograph (Agilent Technologies, Santa Clara, CA, USA) equipped with a DB-5 column (30 m × 0.25 mm × 0.25 μm) and a flame-ionization detector (FID). The amino sugars measured included glucosamine (GluN), mannosamine, galactosamine, and muramic acid (MurA).

Bacterial necromass carbon (BNC) and fungal necromass carbon (FNC) were estimated based on the calculation model established by Hu et al. (2024):

$$BNC = MurA \times 31.3 \quad (5)$$

$$FNC = (GluN - 1.16 \times MurA) \times 10.8 \quad (6)$$

where muramic acid (mg/kg) serves as a specific biomarker for bacteria, while glucosamine (mg/kg) is a common constituent of both fungal and bacterial cell walls.

MNC (mg/kg) is the sum of BNC (mg/kg) and FNC (mg/kg).

$$MNC = BNC + FNC \quad (7)$$

The microbial necromass accumulation coefficient (NAC) refers to the net accumulation of microbial necromass per unit microbial biomass. It was determined with the following equation (Zhang et al., 2021):

$$NAC = MNC/MBC \quad (8)$$

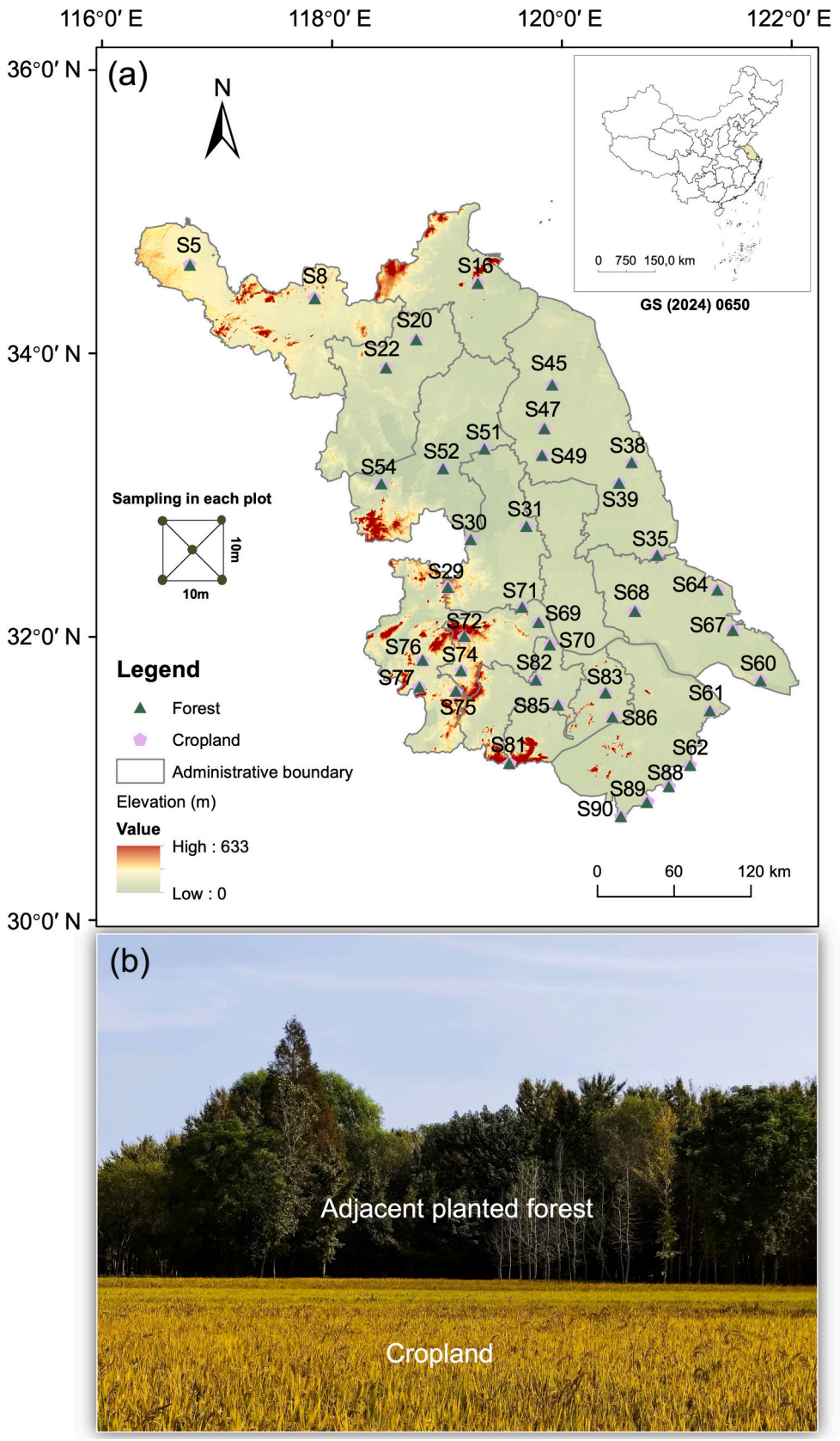

Fig. 1. Location of the study area, (a) the geographic distribution of sampling sites, and (b) general view of the croplands and adjacent planted forests.

2.4. DNA extraction, Illumina sequencing, and sequence processing

Genomic DNA was extracted from cropland and forest soils with the E.Z.N.A.® Soil DNA Kit (Omega Bio-tek, Norcross, GA, USA) according to the manufacturer's instructions. Following extraction, DNA integrity was assessed by 1% (w/v) agarose gel electrophoresis, and its purity and concentration were quantified using a NanoDrop 2000 UV–Vis spectrophotometer. The DNA extracts were stored at −20 °C to preserve stability for downstream analyses.

The bacterial V3-V4 and archaeal V4-V5 hypervariable regions of the 16S rRNA gene were amplified using primer pairs 341F/806R (5′-CCTAYGGGRBGCASCAG-3′ and 5′-GGACTACNNGGGTATCTAAT-3′) and Arch519F/Arch915R (5′-CAGCCGCCGCGGTAA-3′ and 5′-GTGCTCCCCCGCCAATTCCT-3′), respectively. The fungal ITS1 region was amplified with primers ITS1F/ITS2 (5′-CTTGGTCATTTAGAGGAAGTAA-3′ and 5′-GCTGCGTTCTTCATCGATGC-3′).

DNA samples were amplified in triplicate 20-μL reactions containing 4 μL of 5× FastPfu Buffer, 2 μL of 2.5 mM dNTPs, 0.8 μL of each primer (5 μM), 0.4 μL of FastPfu Polymerase, and 10 ng of template DNA. The resulting amplicons were visualized on agarose gels, and bands of the expected size were excised and purified with the AxyPrep DNA Gel Extraction Kit (Axygen Biosciences, Union City, CA, USA). Purified products were subjected to paired-end sequencing (2 × 250 bp) on an Illumina NovaSeq PE250 platform (Shanghai BIOZERON Co., Ltd).

Raw sequencing reads were subjected to stringent quality filtering, discarding sequences shorter than 50 bp, with average quality scores below 20, containing ambiguous bases, or with incorrect primer and barcode matches. Subsequent denoising and inference of amplicon sequence variants (ASVs) were performed using the DADA2 pipeline (Callahan et al., 2016), with paired-end reads trimmed and filtered under a maximum expected error threshold of two. To ensure data quality, singleton ASVs and those assigned to mitochondria or chloroplasts were removed. Bacterial and archaeal ASVs were taxonomically classified against the SILVA database (version SSU138.1) (http://www.arb-silva.de), and fungal ASVs were taxonomically classified against the NCBI-NT database (https://ftp.ncbi.nlm.nih.gov/blast/db/), using the UCLUST algorithm with an 80% confidence threshold. All raw sequences are publicly accessible in the NCBI SRA (http://www.ncbi.nlm.nih.gov/) under BioProject accession numbers PRJNA1280032 (bacteria), PRJNA1280037 (fungi), and PRJNA1280060 (archaea).

2.5. Piecewise structural equation modeling

Piecewise structural equation modeling (piecewiseSEM) was used to discern the direct and indirect effects of PCP (POC, MAOC, DOC) and MDC (MBC, MNC) on SOC in croplands and adjacent planted forests. This method was selected owing to its capacity to deconstruct complex causal networks in correlative data, thereby separating the direct and indirect influences of multiple predictors (Lefcheck, 2016; Liu et al., 2022; Liu et al., 2025a).

We built an a priori model informed by current theory. Its fit was judged via Fisher's C test (with $0.05 < P < 1.00$ indicating a good fit), and we subsequently modified the model by incorporating significant pathways ($P < 0.05$) to improve its overall goodness (Delgado-Baquerizo et al., 2020; Liu et al., 2025a). For all variables included in the final piecewiseSEM, the variance inflation factor (VIF) was confirmed to be below 7.0 (O'brien, 2007). We conducted these analyses using the "piecewiseSEM" package (Lefcheck, 2016) in R.

2.6. Statistical analysis

All data analysis and figure generation were carried out in R software (version 4.5.0) (R Core Team, 2025). We examined differences in soil carbon parameters and properties between croplands and adjacent planted forests using the Wilcoxon test, subsequent to testing for variance homogeneity (Levene's test) and residual normality (Shapiro-Wilk test). Associations between soil microbial communities [bacteria, fungi, archaea, arbuscular mycorrhizal fungi (AMF), and ectomycorrhizal fungi (EcMF)] and carbon parameters were assessed with Mantel tests. Prior to these analyses, soil carbon parameter data were standardized using a Z-score for Euclidean distance computation, while microbial community data were Hellinger-transformed for Bray-Curtis distance calculation.

The Phylogenetic Investigation of Communities by Reconstruction of Unobserved States (PICRUSt2) based on the Kyoto Encyclopedia of Genes and Genomes (KEGG) was used to extrapolate bacterial and archaeal community functions (Langille et al., 2013). The FungalTraits database was employed to predict fungal functional traits, from which AMF and EcMF were identified based on trait classifications for subsequent analysis (Põlme et al., 2020). NMDS1 and NMDS2 were the first and second axis scores of non-metric multi-dimensional scaling (NMDS) ordination, respectively. In our study, the microbial key taxa (MKT) are the top10 abundant taxa of bacteria (phylum), fungi (class), archaea (class), AMF (genus), and EcMF (genus).

To elucidate complex microbial interaction patterns, we established co-occurrence networks for bacteria, fungi, archaea, AMF, and EcMF. Topological attributes of the resulting sub-networks were subsequently extracted to quantify soil microbial network complexity. Prior to network construction, microbial phylotypes exhibiting relative abundances below 0.005% were filtered out. Pairwise associations between ASVs were assessed using Spearman correlation, and the P-values were adjusted by the Benjamini-Hochberg false discovery rate (FDR) test. A significance threshold of FDR-adjusted $P < 0.05$ was applied. Subsequently, only correlations meeting the criteria for robustness ($|r| > 0.50$) and statistical significance were incorporated into the network analysis. We characterized co-occurrence networks using six key topological properties: number of nodes, average weight degree, mean distance, betweenness centralization, network density, and clustering coefficient. Due to significant multicollinearity among these indices, network complexity was quantified using the scores of the first two principal components (Network.PC1 and Network.PC2) derived from a PCA performed on the six properties, following established methodologies (Wang et al., 2023; Liu et al., 2025a).

To assess the influence of various factors on SOC, POC, and MAOC across the different land-use types, we utilized a random forest approach. The models were built with 1000 decision trees (ntree), and their robustness was evaluated through 15-fold cross-validation. The analysis was conducted using the "randomForest" (Liaw and Wiener, 2002) and "rfPermute" (Archer, 2023) packages in R.

3. Results

3.1. Comparative analysis of soil carbon parameters and soil properties in croplands versus adjacent planted forests

Comparative analysis revealed significant differences (Wilcoxon test, $P < 0.05$) in multiple soil carbon parameters between croplands and adjacent planted forests (Fig. 2). SOC, POC, MAOC, MBC, and CSD were significantly higher in croplands. Conversely, DOC/SOC, BNC/SOC, FNC/SOC, and MNC/SOC ratios were elevated in adjacent planted forests. While POC/SOC was higher in croplands and MAOC/SOC was higher in adjacent planted forests, these differences were non-significant (Fig. S2; $P > 0.05$). Crucially, adjacent planted forests exhibited significantly lower CSD than croplands (31.41 ± 10.39% vs. 41.51 ± 16.59%; $P < 0.01$), indicating superior MAOC formation and storage potential in adjacent planted forest soils.

Pronounced contrasts were also observed in soil properties: TP, AP, SWC, NO_3^--N, and EC were significantly higher in croplands (Fig. 2; $P < 0.05$). These divergent hydro-nutrient regimes—driven by agricultural irrigation and fertilization—critically modulated soil microbial activity, community composition, and diversity. This regulation directly influenced DOC bioavailability, thereby governed SOC and its fraction

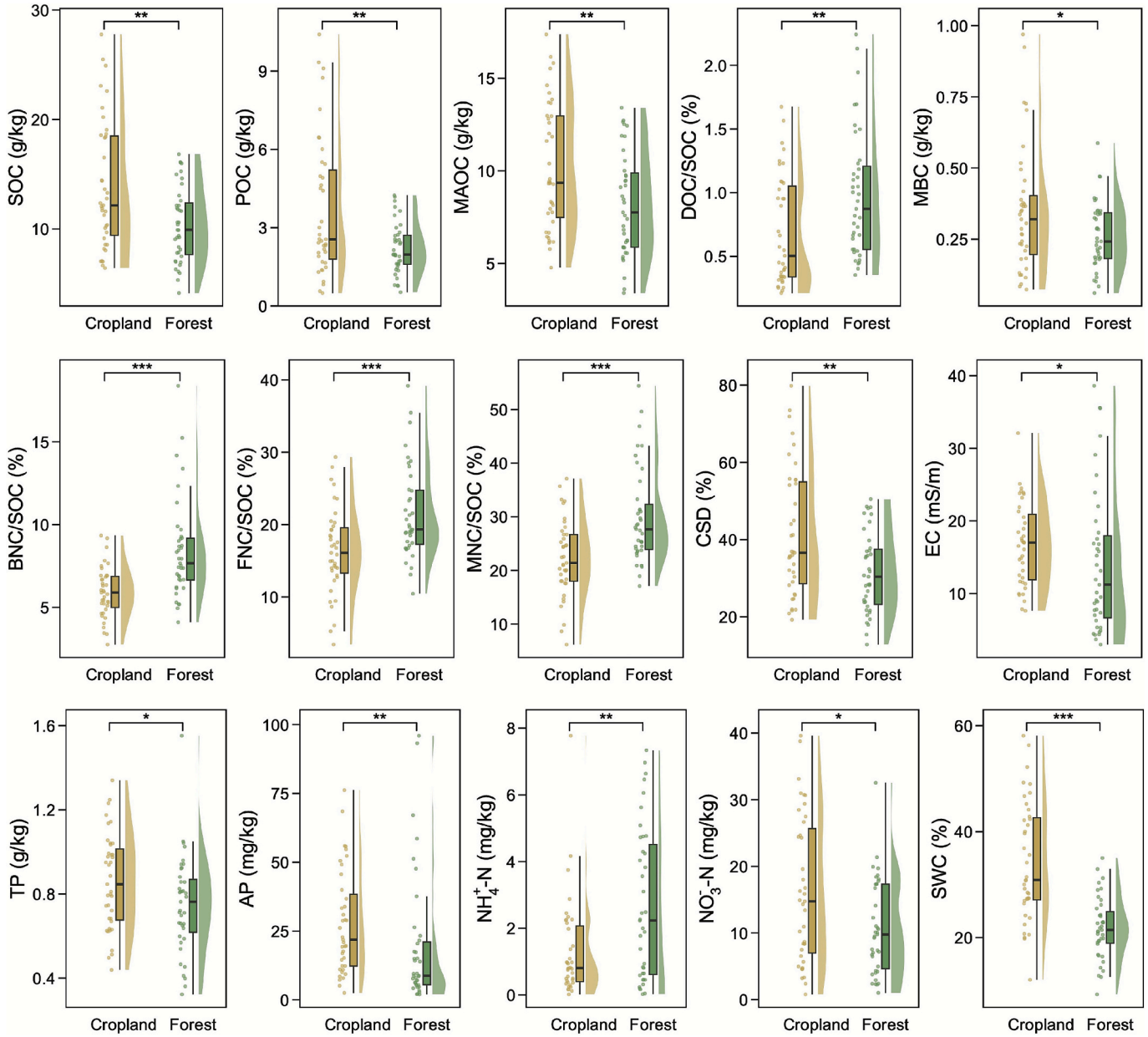

Fig. 2. Differences in soil carbon parameters and soil properties between croplands and adjacent planted forests. DOC/SOC, DOC to SOC ratio; BNC/SOC, BNC to SOC ratio; FNC/SOC, FNC to SOC ratio; MNC/SOC, MNC to SOC ratio. The differences were tested using Wilcoxon test (*: $P < 0.05$, **: $P < 0.01$, ***: $P < 0.001$).

contents. The lower bioavailability of DOC in adjacent planted forests also contributed to their significantly higher DOC/SOC ratio compared to croplands (Fig. 2).

3.2. Linkages between soil carbon parameters and microbial communities

We conducted Mantel tests to examine the linkages between soil carbon parameters and microbial communities. Overall, SOC, POC, MAOC, and CSD were positively correlated with the community composition of bacteria, fungi, archaea, and EcMF in croplands (Fig. 3a; $p < 0.05$). POC/SOC and MAOC/SOC were positively correlated with the community composition of AMF and EcMF in croplands (Fig. 3a; Mantel's $r = 0.1$–0.4, $p < 0.05$). DOC and DOC/SOC were positively correlated with the community composition of bacteria and fungi in croplands (Fig. 3a; Mantel's $r > 0.2$, $p < 0.01$). In contrast, DOC and DOC/SOC were correlated with microbial community composition to a lesser degree in adjacent planted forests (Fig. 3b; Mantel's $r < 0.1$, $p > 0.05$).

SOC, MAOC, and CSD were positively correlated with the community composition of bacteria, fungi, archaea, and AMF in adjacent planted forests (Fig. 3b; Mantel's $r = 0.1$–0.4, $p < 0.01$). Notably, POC, $MAOC_{max}$, and MBC were correlated with microbial community composition to a lesser degree in adjacent planted forests ($p > 0.05$). NAC was positively correlated with the microbial community composition in adjacent planted forests (Fig. 3b; Mantel's $r = 0.1$–0.4, $p < 0.01$).

MKT showed significant positive correlations ($P < 0.05$) with SOC, POC, and MAOC across different land-use types. In croplands, these correlations occurred with Tremellomycetes (fungal class), Nanoarchaeia (archaeal class), *Paraglomus* (AMF's genus), and *Tarzetta* (EcMF's genus) (Fig. S3a), while adjacent planted forests exhibited correlations with Firmicutes (bacterial phylum), Glomeromycetes (fungal class), Archaeorhizomycetes (fungal class), and *Paraglomus* (AMF's genus) (Fig. S3b).

We also examined the linkages in soil carbon parameters and found

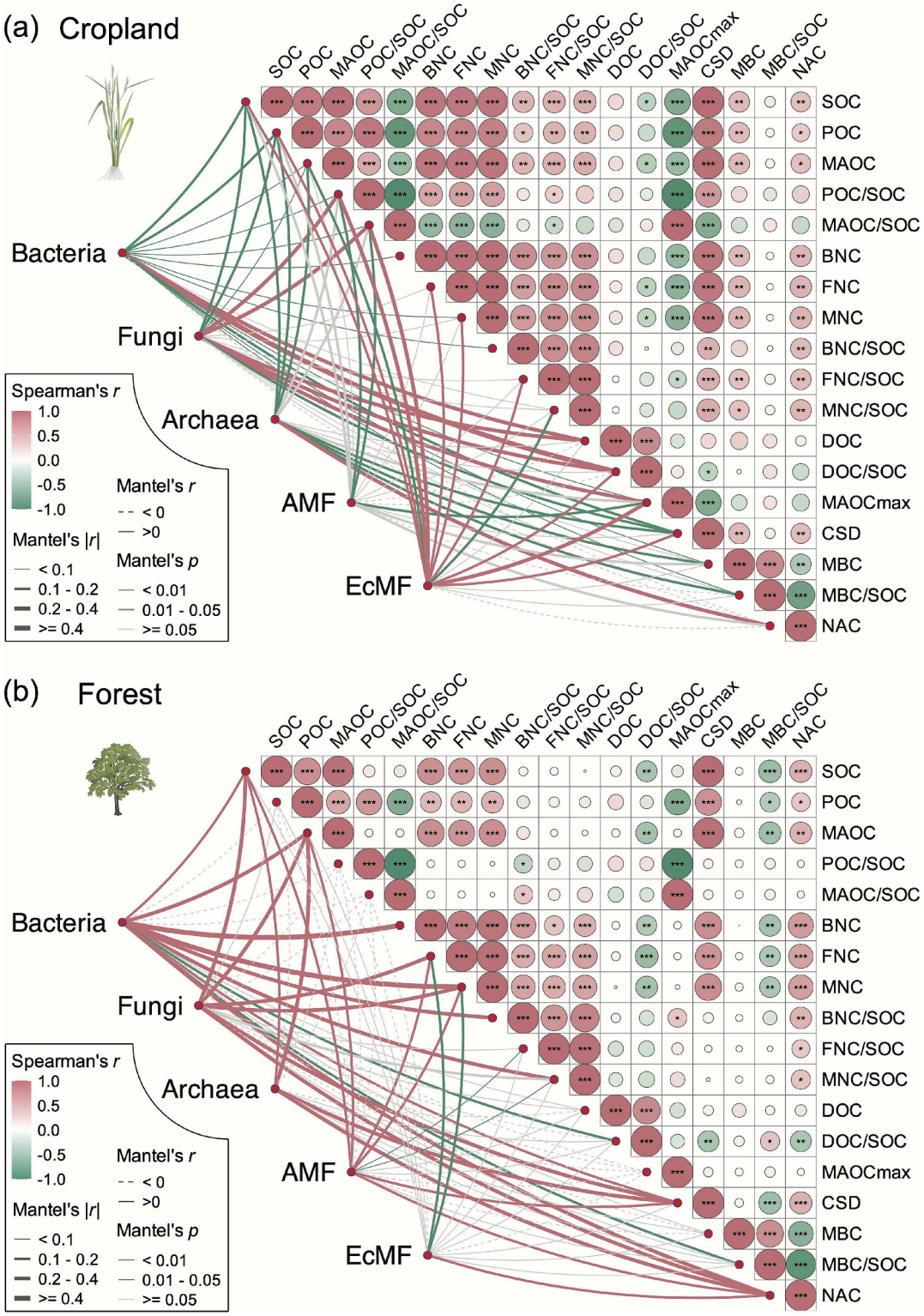

Fig. 3. Associations of soil carbon parameters with soil microbial communities (bacteria, fungi, archaea, AMF, and EcMF) in (a) croplands and (b) adjacent planted forests. Pairwise comparisons of soil carbon parameters are shown at the upper-right, with a color gradient representing Spearman's correlation coefficients. Soil microbial community composition was correlated to each carbon parameters by partial Mantel tests. The line width represents the partial Mantel's *r* statistic for the corresponding correlation, and line color means that significances are tested based on 999 permutations. The solid line represents positive correlation, and dashed line represents negative correlation. POC/SOC, POC to SOC ratio; MAOC/SOC, MAOC to SOC ratio; BNC/SOC, BNC to SOC ratio; FNC/SOC, FNC to SOC ratio; MNC/SOC, MNC to SOC ratio; DOC/SOC, DOC to SOC ratio; MBC/SOC, MBC to SOC ratio. *: $P < 0.05$, **: $P < 0.01$, ***: $P < 0.001$.

that SOC, POC, and MAOC were markedly positively correlated with BNC, FNC, MNC, BNC/SOC, FNC/SOC, MNC/SOC, CSD, MBC, and NAC in croplands (Fig. 3a; Spearman's $P < 0.05$). However, SOC, POC, and MAOC were markedly positively correlated only with BNC, FNC, MNC, CSD, and NAC in adjacent planted forests (Fig. 3b; Spearman's $P < 0.05$). Furthermore, SOC, POC, and MAOC demonstrated significant positive associations with bacterial sub-network topology properties in croplands (Fig. S4a), but correlated more strongly with fungal and archaeal sub-network properties in adjacent planted forests (Fig. S4b).

3.3. Quantifying the importance of major drivers for SOC, POC, and MAOC in croplands and adjacent planted forests

Random forest analyses revealed fundamental divergence in driver dominance between croplands and adjacent planted forests. In croplands, PCP (summed relative importance value = 41.05%) dominated SOC regulation, markedly surpassing biotic drivers (24.80%) and MDC (22.76%), while abiotic factors showed minimal contributions (Fig. 4a). In adjacent planted forests, abiotic drivers (30.98%) outweighed biotic drivers (19.16%) for SOC, with MDC (15.04%) being marginal (Fig. 4b). Furthermore, CSD (16.32%) among PCP, soil properties (SP) (22.12%) among abiotic drivers, and microbial network topology properties (MN, containing microbial community structure properties) (10.63%) among biotic drivers showed high relative importance for SOC in adjacent planted forests (Fig. 4b).

CSD, MAOC, POC, BNC, MNC, and TN exhibited markedly high relative importance for SOC in croplands and adjacent planted forests within the top 35 drivers (Fig. 4a and b; $P < 0.01$). Notably, FNC exhibited markedly higher relative importance for SOC in croplands (Fig. 4a) than in adjacent planted forests (Fig. 4b). Moreover, MAOC/SOC, $MAOC_{max}$, EcMF *Jimgerdemannia*, POC/SOC, and Archaea Thermoplasmata also exhibited high relative importance for SOC in croplands (Fig. 4a; all relative importance value >3.50%). Contrastingly, silt and NO_2 exhibited markedly high relative importance for SOC in adjacent planted forests (Fig. 4b).

In croplands, MDC (29.74%) and PCP (29.66%) collectively showed markedly high and similar relative importance for MAOC, both exceeding biotic (21.19%) and abiotic drivers (19.41%) (Fig. 4c). Notably, biotic drivers outweighed abiotic drivers for MAOC. Furthermore, CSDx (19.50%) among PCP, SP (14.56%) among abiotic drivers, and MN (11.59%) among biotic drivers showed high relative importance for MAOC in croplands (Fig. 4c). In adjacent planted forests, abiotic drivers (42.56%) dominated MAOC regulation, markedly surpassing biotic drivers (20.44%) and MDC (19.96%), while PCP showed minimal contributions (17.04%), indicating fundamental divergence in carbon stabilization mechanisms between land-use types (Fig. 4d). Furthermore, SP (29.42%) among abiotic drivers, MN (9.75%) among biotic drivers, MNCx (7.76%) among MDC, and CSD (17.04%) among PCP showed high relative importance for MAOC in adjacent planted forests (Fig. 4d).

CSD, MNC, BNC, FNC, and TN exhibited markedly high relative importance for MAOC in croplands and adjacent planted forests within the top 35 drivers (Fig. 4c and d; all *P*-values less than 0.05). Notably, POC exhibited markedly higher relative importance for MAOC in croplands (Fig. 4c) than in adjacent planted forests (Fig. 4d). Moreover, TWI, POC/SOC, $MAOC_{max}$, and POC/SOC also exhibited high relative importance for MAOC in croplands (Fig. 4c; all relative importance value >3.48%). Contrastingly, silt, NO_2, Cu, average weight degree of archaea, MAT, elevation, and pH exhibited markedly highe relative importance for MAOC in adjacent planted forests (Fig. 4d). The highest relative importance of CSD for SOC and MAOC indicates that mineral association is the primary pathway for stabilizing SOC, yet its capacity is finite. In soils approaching or reaching saturation, the mineral sorption capacity becomes the prime constraint on SOC accumulation and stability.

Land-use dictated the driver hierarchy, with biotic drivers collectively exhibiting higher relative importance for POC than abiotic drivers in croplands, while adjacent planted forests displayed the reverse dominance pattern (Fig. S5). In croplands, biotic drivers (33.71%) and MDC (32.40%) collectively dominated POC regulation, surpassing abiotic drivers (30.89%), while PCP (i.e., DOC) showed minimal contributions (Fig. S5a). In adjacent planted forests, abiotic drivers (45.91%) dominated POC regulation, markedly surpassing biotic drivers (34.49%) and MDC (17.65%), while PCP (i.e., DOC) also showed minimal contributions (Fig. S5b). Furthermore, it showed that FNC and MNC were the most important variables of POC in croplands (Fig. S5a) and TN was the most important variable of POC in adjacent planted forests (Fig. S5b).

Further analysis revealed that SOC, MAOC, and POC in croplands increased significantly with the increase of TN, TN/TP, SWC, and NO_2 (Figs. 5 and S6; $P < 0.05$). While in adjacent planted forests, SOC and MAOC increased significantly with the increase of TN, NO_2, Cu, and Silt (Fig. 5; $P < 0.01$). Conversely, SOC, MAOC, and POC in croplands decreased significantly with the increase of pH and SBD (Figs. 5 and S6; $P < 0.01$). While in adjacent planted forests, SOC and MAOC only decreased significantly with the increase of pH (Fig. 5; $P < 0.01$).

3.4. Exploration of direct and indirect effects of PCP and MDC on SOC in croplands and adjacent planted forests

PiecewiseSEM results showed that SOC was directly significantly influenced by POC (path coefficient was 0.45, $R^2 = 0.67$, $P < 0.001$) and MAOC (path coefficient was 0.59, $R^2 = 0.83$, $P < 0.001$) in croplands (Fig. 6a). DOC, MBC, and MNC had positive indirect effects on SOC. Notably, the positive effects of POC and MAOC on SOC were similar in croplands (Fig. 6a). The total positive effect of MNC (standardized effect was 0.89) on SOC was the largest, followed by POC (standardized effect was 0.67) in croplands (Fig. 6c). The total positive effects of MAOC (standardized effect was 0.59) and MBC (standardized effect was 0.43) on SOC were also high (Fig. 6c).

SOC was also directly significantly influenced by POC (path coefficient was 0.28, $R^2 = 0.19$, $P < 0.001$) and MAOC (path coefficient was 0.81, $R^2 = 0.57$, $P < 0.001$) in adjacent planted forests (Fig. 6b). Notably, MNC exerted a 27.27% stronger promotion on MAOC than on POC in adjacent planted forests, and this MAOC increment subsequently reinforced SOC accrual with a 2.89-fold higher contribution than POC-derived pathways. The total positive effect of MAOC (standardized effect was 0.81) on SOC was the largest, followed by MNC (standardized effect was 0.69) in adjacent planted forests (Fig. 6d). The total positive effect of POC (standardized effect was 0.54) on SOC was also high. MBC and DOC had less of a total positive effect on SOC (Fig. 6d; total effect <0.01).

Crucially, DOC exerted 40.74% stronger promotion on MBC in croplands than in adjacent planted forests, and DOC exerted a 71.37-fold stronger promotion on SOC accrual in croplands than in planted forests (Fig. 6), establishing DOC as the keystone driver of cropland carbon sequestration. This divergence primarily stemmed from the superior hydro-nutrient conditions in croplands, which enhanced microbial activity and carbon sequestration capacity. Consequently, elevated DOC bioavailability fueled more efficient microbial processing—notably via higher microbial carbon pump efficiency—ultimately establishing divergent SOC formation and stabilization pathways relative to adjacent planted forests.

4. Discussion

4.1. Divergent SOC patterns and their underlying abiotic drivers between croplands and adjacent planted forests

We found significantly higher SOC in croplands than in adjacent planted forests, supporting the concept of elevated SOC storage potential in agricultural systems mediated by stoichiometry and microbial

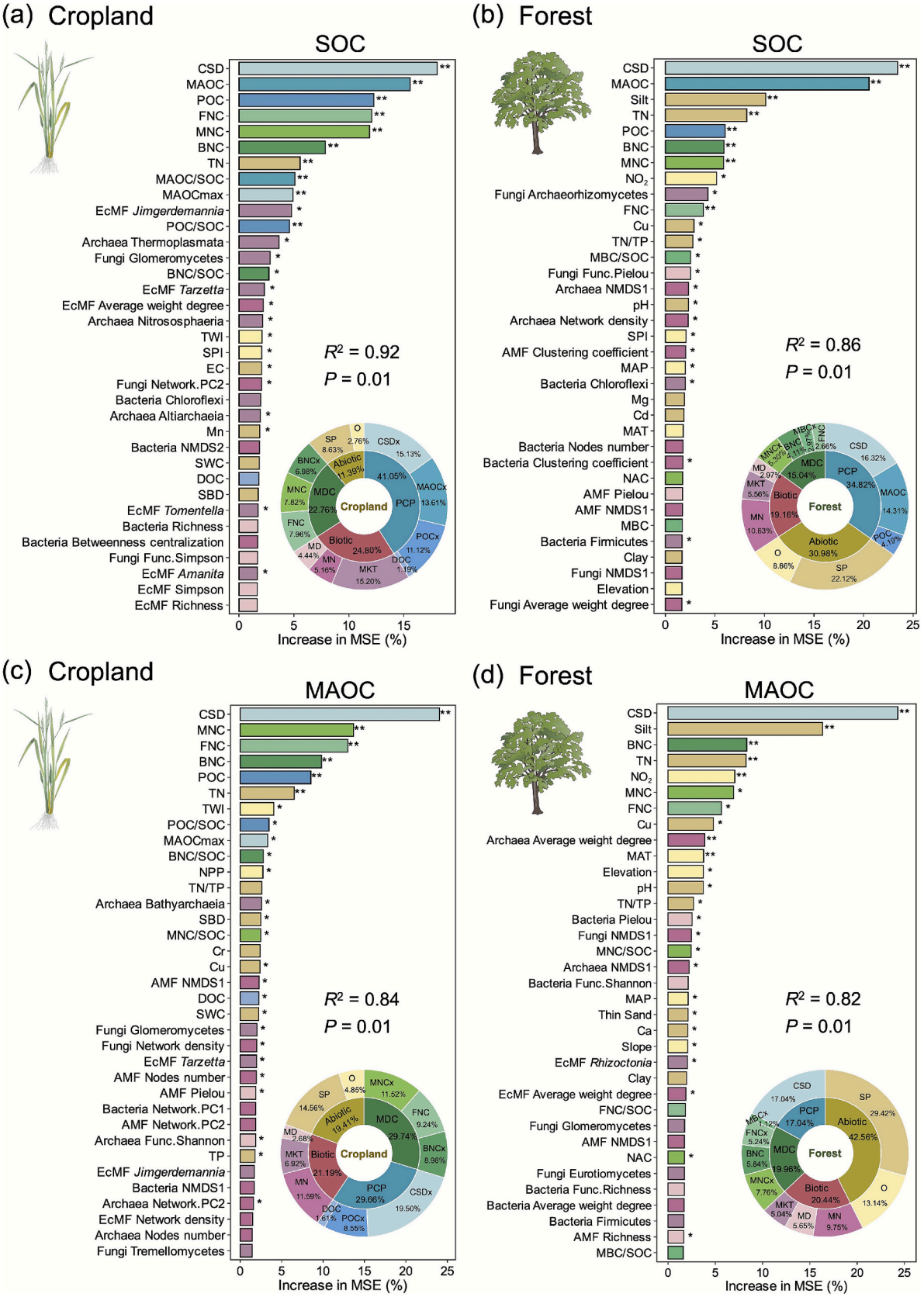

(caption on next page)

Fig. 4. Relative importance of physical carbon parameters, biotic-abiotic drivers, and microbial-derived carbon for SOC and MAOC in (a, c) croplands and (b, d) adjacent planted forests. MSE, percentage of increase of mean square error (%). Bars marked with "*", "**", and "***" represent variables that are significant at the <0.05, <0.01 and <0.001 level, respectively. R^2 and P values are the variance explained (i.e., goodness of fit) and significance of the random forest model. PCP, physical carbon parameters; SP, soil properties; O, Others (e.g., climate, terrain, vegetation factors, etc.); MDC, microbial-derived carbon; MKT, microbial key taxa (i.e., top10 abundant taxa); MN, microbial network topology properties, containing microbial community structure properties; MD, microbial community taxonomic and functional diversity; NMDS1, first axis scores of NMDS; NMDS2, second axis scores of NMDS; Network.PC1, first principal component extracted using sub-network topology properties; Network.PC2, second principal component extracted using sub-network topology properties; Func., functional; POC/SOC, POC to SOC ratio; MAOC/SOC, MAOC to SOC ratio; BNC/SOC, BNC to SOC ratio; FNC/SOC, FNC to SOC ratio; MNC/SOC, MNC to SOC ratio; MBC/SOC, MBC to SOC ratio; TN/TP, TN to TP ratio; CSDx, CSD and/or $MAOC_{max}$; MAOCx, MAOC and/or MAOC/SOC; POCx, POC and/or POC/SOC; BNCx, BNC and/or BNC/SOC; FNCx, FNC and/or FNC/SOC; MNCx, MNC and/or MNC/SOC; MBCx, MBC and/or MBC/SOC.

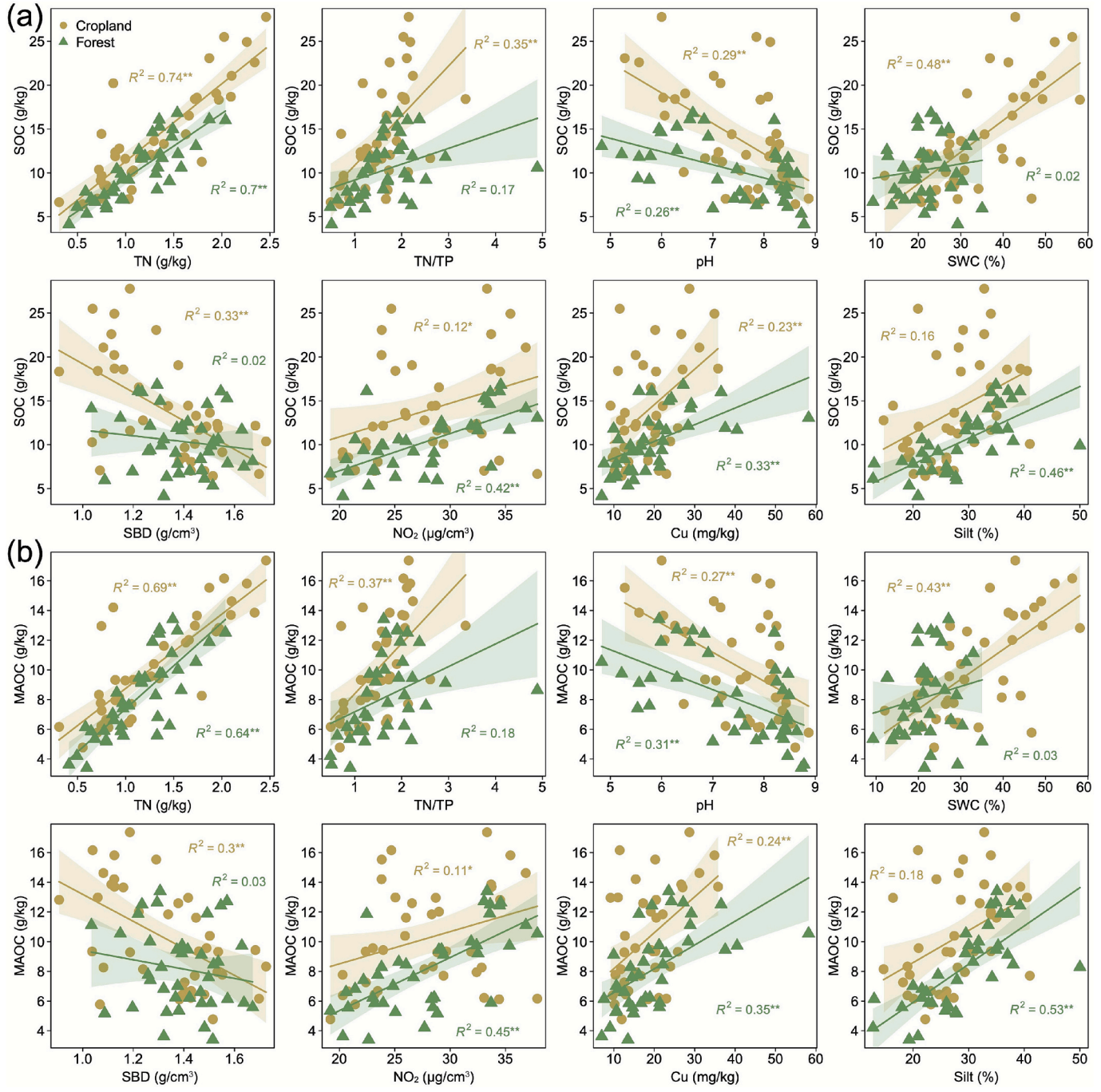

Fig. 5. Differential responses of (a) SOC and (b) MAOC contents to major abiotic drivers in croplands versus adjacent planted forests. The solid line represents the trends, and the shaded area represents the standard error of the estimate. TN/TP, TN to TP ratio. *: $P < 0.05$, **: $P < 0.01$.

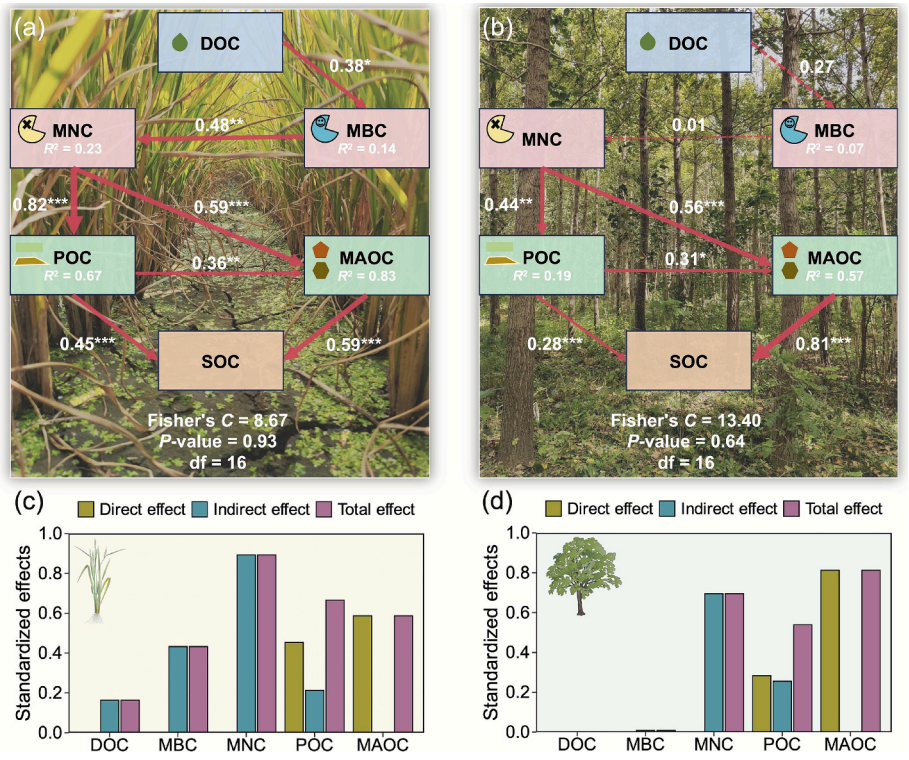

Fig. 6. Piecewise structural equation modeling (piecewiseSEM) accounting for the direct and indirect effects of physical carbon parameters (DOC, POC, and MAOC) and microbial-derived carbon (MBC, MNC) on SOC in (a, c) croplands and (b, d) adjacent planted forests. Numbers adjacent to arrows are path coefficients (partial regression) which represent the directly standardized effect size of the relationship. The standardized path coefficients in the paths are shown in red if positive. Significant paths ($P < 0.05$) are represented by solid lines, and non-significant paths ($P > 0.05$) are represented by dashed lines in the figure. Significance levels of each predictor are $^{*}P < 0.05$, $^{**}P < 0.01$, $^{***}P < 0.001$. Standardized effects (total, direct, and indirect effects) based on piecewiseSEM are shown in the figure at the bottom. df, degree of freedom.

metabolism (Wang et al., 2024a). This divergence is driven by contrasting mechanisms: croplands benefit from nutrient inputs and straw retention, while forests experience carbon loss from limited litter inputs and high C:N residues. A key factor was SWC, which significantly correlated with SOC in croplands (Fig. 5a; $R^2 = 0.48$, $P < 0.01$) but not in forests. This is consistent with established SWC-SOC coupling mechanisms in agriculture (Wang et al., 2023; Liu et al., 2025a). This contrasting role of SWC may stem from fundamental differences in ecosystem functioning. In croplands, frequent irrigation and fertilization maintained optimal and relatively stable SWC. This not only increased nutrient availability but also promoted continuous root growth and exudation, providing a steady flow of labile carbon substrates (e.g., sugars, organic acids) that fueled the microbial carbon pump and facilitated SOC formation (Sokol and Bradford, 2019; Wang et al., 2021). Therefore, SWC acted as an integrator, regulating the entire chain of biotic processes from substrate availability to microbial efficiency that underpinned SOC accrual. This was supported by previous research, which identified SWC as having significant relative importance for SOC storage in paddy fields (Liu et al., 2025a). In contrast, the adjacent planted forests experienced more variable natural precipitation and lack irrigation. More importantly, their lower disturbance and different litter quality likely led to a microbial community with different physiological strategies and a greater dependence on sporadic, recalcitrant carbon inputs. Under these conditions, SWC might have become a less limiting factor compared to carbon substrate quality and microbial community composition, shifting the dominant controls toward abiotic stabilization pathways (e.g., mineral association) and explaining its weaker predictive power for SOC in planted forests.

Different with our findings, Li et al. (2025b) reported higher SOC content in forest ecosystems compared to cropland ecosystems within the 0–20 cm soil layer. This divergence can be attributed to distinct environmental contexts and management histories. Their study was conducted in a semi-humid continental monsoon climate zone of Northern China (MAP = 641 mm, MAT = 6.9 °C), focusing on continuous rainfed maize systems and adjacent poplar forests. In contrast, our regional-scale investigation spanned the subtropical humid monsoon climate of Eastern China (MAP = 989.9 ± 103.54 mm, MAT = 15.78 ± 0.63 °C), where croplands were dominated by paddy rice or rice-wheat rotations with a long history of intensive management including irrigation and fertilization. Moreover, the dominant tree species of the adjacent planted forests in our study is the *Populus* spp. (stand age approximately 15 ± 5 years). Furthermore, differential soil textural compositions likely contribute to these contrasts. Their study area displayed mean sand/silt/clay ratios of 21.7%/51.7%/26.7%, dominated by silt, while both cropland and forest soils in our regional analysis exhibited a more balanced texture averaging 36.6%/28.2%/35.2% (sand/silt/clay, respectively). Our random forest analysis confirmed silt content as a significant SOC driver in adjacent planted forests (third-ranked variable, $P < 0.01$), underscoring soil texture coupled with the contrasting climate and cropping systems (rainfed maize systems vs. rice paddies), can fundamentally alter the relative SOC storage potential of croplands versus forests. Notably, the soils in the study by Li et al. (2025b) were classified as Mollisols, dominated by 2:1 expanding clay minerals (particularly montmorillonite). In contrast, the soils in our study have a long-term land-use history as paddy fields, dating back to at least the 1980s. Although located within a transitional clay mineral zone (illite-vermiculite-kaolinite), these soils are mainly characterized by 1:1 clay minerals and active iron oxides as their dominant components (Wei et al., 2021). Meanwhile, the minor 2:1 clay minerals have been either transformed into 1:1 clay minerals or degraded due to prolonged intense leaching and paddy management.

Although croplands are often reported to contain less SOC than

forests, especially natural forests (Dor et al., 2025; Gong et al., 2025), our research in a subtropical floodplain ecosystem revealed the opposite pattern. We proposed that this was primarily due to the high inherent SOC capacity of rice-based systems (Wei et al., 2021; Li et al., 2022; Wu et al., 2024), which fundamentally differ from the rainfed grain systems of comparative studies. Whereas SOC recovery in planted forests was described as a gradual process driven by litter accumulation (Zhang et al., 2023), the croplands in our study benefited from optimized hydro-nutrient conditions and substantial carbon inputs from straw and root exudates. This management combination effectively created a regime of productive disturbance and favorable biogeochemistry, thereby supporting higher SOC storage in croplands than in the less-disturbed but potentially nutrient- or water-limited adjacent planted forests. This finding confirms our first hypothesis.

4.2. *Higher SOC stability in adjacent planted forests mediated by MAOC, while DOC, MDC, and biotic factors dominated in croplands*

We found that SOC accumulation involved a substantial dual contribution from POC and MAOC in croplands, whereas MAOC dominated in planted forests. This divergence can be explained by the lower CSD in adjacent planted forests, which favors the progressive stabilization of MAOC (Cotrufo and Lavallee, 2022; Breure et al., 2025). Additionally, substantial input from crop residue return and green manure in croplands may have led to a higher proportion of POC (Cotrufo et al., 2022). Concurrently, the reduced litter input in forests results in a smaller relative contribution of POC to SOC. Consistently, the higher MAOC/SOC ratio in planted forests (Fig. S2) indicates enhanced SOC stability (Liu et al., 2025b), aligning with global observations that MAOC dominates in lower-carbon forest soils (Cotrufo et al., 2019) and in subtropical forests specifically (Chen et al., 2023). Previous studies have found that a higher proportion of SOC in paddy soils is stored as microaggregate-protected POM (Denef et al., 2007; Wei et al., 2021). This storage mechanism leads to lower stability of SOC in paddy fields relative to adjacent planted forests, thereby confirming our second hypothesis.

Furthermore, our analyses revealed that DOC and MBC significantly mediated the formation of POC, MAOC, and SOC in croplands. This likely stems from the fact that DOC in croplands is predominantly derived from labile root exudates, easily decomposable residues, or farmyard manure, green manure, and compost, which, under optimized hydro-nutrient conditions, are efficiently utilized by microorganisms to drive the microbial carbon pump (Cotrufo et al., 2013; Cotrufo and Lavallee, 2022; Wang et al., 2025a). This is consistent with the understanding that DOC serves as an efficient precursor for SOC, entering both MAOC and POC pools through microbial processing (Cotrufo and Lavallee, 2022; Si et al., 2024). Previous research has also found that the altered soil microenvironment in paddy fields significantly promotes microbial activity, leading to the release of DOC from microbial cells into the soil (Wang et al., 2025a). In contrast, these pathways were less pronounced in planted forests. Here, DOC originates more from the leaching of recalcitrant, high C:N litter (e.g., leaves), which provides sporadic, less bioavailable carbon substrates (Magill and Aber, 2000; Michalzik et al., 2001). Coupled with lower SWC, N and P availability, and reduced microbial activity, the transformation of this litter-derived DOC into microbial biomass and stable carbon pools is strongly constrained, explaining its weaker contribution to SOC formation in planted forests (Xiao et al., 2023; Huang et al., 2024). This confirms our third hypothesis that the contribution of DOC to SOC formation and stabilization differs between croplands and adjacent planted forests.

We found that biotic factors (e.g., MKT) and MDC (e.g., MNC, BNC, FNC) had a higher influence on SOC in croplands than in planted forests, with specific taxa (e.g., *Jimgerdemannia*, Thermoplasmata, Glomeromycetes) being particularly influential. This likely results from intensified microbial growth and decomposition processes in croplands, fueled by rhizodeposits and litter inputs (Wang et al., 2021). Fertilization may further enhance microbial carbon use efficiency while reducing extracellular enzyme activity and respiration (Sun et al., 2025), whereas nutrient limitation in forests constrains microbial efficiency and carbon accumulation (Wang et al., 2024a). The consistent positive MBC-SOC correlation confirms the critical microbial pathway in croplands (Xu et al., 2013; Crowther et al., 2019; Li et al., 2024). The observed divergence in FNC and BNC contributions between croplands and planted forests likely stems from fundamental differences in microbial life history strategies, mortality pathways, and environmental stress regimes. In croplands, the dominance of FNC can be attributed to a synergy of factors. Abundant and labile carbon inputs from rhizodeposits and residues, coupled with stable hydro-nutrient conditions from irrigation and fertilization, support vigorous fungal growth and high turnover rates of their extensive hyphal networks (Sokol and Bradford, 2019; Kan et al., 2025). Fungal mortality, through processes such as hyphal fragmentation, provides a continuous stream of necromass. This necromass is inherently recalcitrant due to chemical composition, rich in chitin and melanin, and is further stabilized through physical protection within soil aggregates promoted by the hyphal networks themselves (Kan et al., 2025). Previous studies on agriculture also demonstrated that the contribution of FNC to SOC was significantly greater than that of BNC (Tian et al., 2024; Kan et al., 2025). Another study focusing on global cropland topsoils also reported a higher contribution of FNC to SOC (Liu et al., 2024), which supports our findings.

Conversely, the greater relative importance of BNC in adjacent planted forests may be driven by a contrasting set of conditions. Lower substrate quality from high C:N litter, coupled with poor hydro-nutrient conditions and periodic moisture stress from variable precipitation, constrains fungal hyphal development and activity (Wang et al., 2024b). In this context, bacteria, with their rapid response to sporadic labile carbon pulses, may become more prominent. A previous study revealed that, compared to fungi, which preferentially utilize plant-derived compounds, a broader range of bacteria may possess the ability to decompose fungal biomass (López-Mondéjar et al., 2018). Crucially, the stabilization pathway in forests shifts toward stronger mineral-organic associations. Bacterial necromass, rich in peptidoglycan and amine groups, has a high affinity for mineral surfaces such as clays and iron oxides. In mineral-dominated pathways, this efficient chemical stabilization, coupled with a greater abundance of macroaggregate-occluded microaggregates, likely enhances the relative contribution of BNC to the persistent SOC pool in forest soils (Denef et al., 2007; Zhao et al., 2025a). A previous study on subtropical forests found that drought reduces the contribution of FNC to MNC while increasing the contribution of BNC, thereby making BNC more important than FNC in SOC accumulation (Wang et al., 2024b). This shift in contribution aligns with our finding that BNC contributes more to SOC in planted forest soils with lower soil water content.

4.3. *MAOC dominated by abiotic factors in adjacent planted forests versus POC and MAOC influenced by MDC and biotic factors in croplands*

We observed a clear pattern of higher POC and MAOC in croplands compared to adjacent planted forests. Environmental stresses (e.g., hypoxia) caused by seasonal flooding inhibit the ability of microorganisms to decompose organic matter, leading to incomplete decomposition and accumulation of plant residues, which can result in higher POC levels in rice paddies (Chen et al., 2021). Moreover, flooding leads to less stable agglomerates (e.g., frequent wet/dry interchanges destroying large agglomerates), and the released organic residues are more likely to be stored temporarily as POC. Forest soils are drier than cropland soils, and the higher oxygen content of their soils promotes rapid decomposition of plant residues by microorganisms, which are then converted more to MAOC or mineralised to CO_2 through microbial metabolism, with less accumulation of POC (Chen et al., 2021). We also found a significant correlation between MNC and POC in croplands and adjacent planted forests, and that MNC had a greater effect on POC in

croplands than in adjacent planted forests. This finding is supported by a previous study, which reports that MNC may be more effective at enhancing POC compared to MAOC (Yang et al., 2025). CSD and MDC (e.g., MNC) exhibited high relative importance for MAOC in both croplands and planted forests. Furthermore, in croplands, POC also showed a strong influence on MAOC, likely because POM surfaces act as hotspots for microbial activity and the formation of MAOC, thereby regulating SOC persistence (Witzgall et al., 2021). A previous study demonstrated a significant positive correlation between MAOC and MNC (Li et al., 2024). King and Sokol (2025) showed that CSD deficit increases new MAOC formation. Their study further established that the concentration or flux rate of DOC inputs regulates MAOC formation efficiency by modulating the partitioning between microbial assimilation and direct mineral sorption pathways.

Our study found that AMF and EcMF had nonnegligible effects on POC and MAOC in croplands, but their influence was comparatively limited in adjacent planted forests (Tables S1 and S2). Notably, although both AMF and EcMF jointly influenced the storage of POC and MAOC in croplands, AMF contributed more to MAOC, and EcMF contributed more to POC. Under the anaerobic stress of paddy field flooding, EcMF dispersing from adjacent planted forests may mediate the decomposition of recalcitrant residues by secreting enzymes that function under low-oxygen conditions. This allows them to preferentially utilize the abundant fresh or partially decomposed POM that accumulates during flooding, thereby securing early access to POC precursor resources. Thus, this relatively inefficient anaerobic process probably promotes both the accumulation and turnover of POC (Li et al., 2025a). In contrast, AMF may contribute to the MAOC pool through two principal mechanisms. First, their hyphal networks and secreted compounds (e.g., glomalin) serve as key biological agents for forming and stabilizing soil macro-aggregates (Wilson et al., 2009; de Goede et al., 2025; Zhao et al., 2025b). The physical encapsulation of organic matter within these aggregates represents a core mechanism for long-term MAOC stabilization, although frequent tillage can partially diminish this benefit. Furthermore, the rapid turnover of AMF hyphae generates substantial necromass (Raffa et al., 2025). This necromass is inherently chemically stable and probably binds to clay mineral surfaces via hydrogen bonding and ionic interactions, facilitating its direct integration and stabilization within the MAOC pool.

In contrast, abiotic factors—including silt, TN, NO_2^--N, Cu, MAT, elevation, and pH—collectively contributed 42.56% to MAOC variation in planted forests. This aligns with global patterns where fine particles (clay+silt), pH, and elevation are key predictors of MAOC (Zhou et al., 2024), as higher silt and clay content provides more mineral surfaces for organo-mineral bonding (Six et al., 2002; Haddix et al., 2020). Furthermore, significant positive associations between MAOC and both atmospheric nitrogen deposition (consistent with a meta-analysis by Tang et al., 2023) and MAT (relative importance: 3.76%) were observed. The positive effect of MAT is corroborated by studies showing increased MAOC under warming conditions (Zhang et al., 2025). The integrated results and above discussions confirm our fourth hypothesis that SOC and its fractions are influenced by distinct mechanisms in croplands versus adjacent planted forests, driven by habitat-specific soil-microbe-plant-environment interactions.

4.4. Implications, limitations, and future directions

Our study establishes land-use-specific mechanisms in regional soil carbon regulation. Croplands, with higher CSD, maintain MAOC pools near saturation, while adjacent planted forests (lower CSD) possess greater residual MAOC capacity. The greater reliance on POC for SOC accumulation in croplands results in a larger but less stable carbon stock, exhibiting heightened vulnerability to environmental perturbations such as warming and tillage due to POC's faster turnover (Fig. 7), highlighting a critical trade-off between SOC content and stability.

Our findings call for land-use-specific management frameworks. In croplands, management strategies should aim to enhance the POC pool by increasing external carbon inputs and minimizing soil disturbance (Angst et al., 2023; Li et al., 2024). Effective measures include deep straw incorporation, combined application of biochar and inorganic fertilizers, cultivation of green manures, and adoption of conservation tillage such as reduced- or no-tillage (Cotrufo and Lavallee, 2022; Kan et al., 2025; Mi et al., 2025; Zhou et al., 2025). For adjacent planted forests, management should aim to rapidly build the MAOC pool by creating optimized hydro-nutrient conditions (Castellano et al., 2015; Craig et al., 2021; Li et al., 2024). Practical measures include ensuring supplemental irrigation during the early establishment phase and dry seasons to secure survival and growth, applying organic-inorganic compound fertilizers, and planting diverse tree species (including nitrogen-fixing varieties) to improve soil health (He et al., 2025). In the socio-economic context of densely populated Eastern China with limited land resources, implementing these measures requires acknowledging trade-offs, such as balancing short-term input costs against long-term ecological benefits. Therefore, appropriate policy incentives are crucial to encourage adoption. Ultimately, integrated accounting of both above- and below-ground carbon pools remains essential for accurate ecosystem carbon assessment and management, particularly as soil carbon dynamics may not parallel the increases in aboveground carbon stocks following afforestation (Cheng et al., 2024).

Several limitations warrant acknowledgment. First, our study area is situated within a transitional clay mineral zone (illite-vermiculite-kaolinite), but these soils are mainly characterized by 1:1 clay minerals. Therefore, depending on soil texture and mineral characteristics, the $MAOC_{max}$ or CSD calculated based on previous empirical equations may be overestimated or underestimated with uncertainty. The conventional view posits a lower $MAOC_{max}$ for soils rich in low-surface-area 1:1 clay minerals like kaolinite, compared to those dominated by high-surface-area 2:1 clay minerals such as montmorillonite and illite (Kleber et al., 2021; Georgiou et al., 2022; Song et al., 2025). However, this apparent limitation of 1:1 clay minerals can be offset by the presence of Fe- and Al-oxides on their surfaces, which provide reactive sites that foster strong organo-mineral bonding and enhance microaggregate stability (Kaiser and Guggenberger, 2003). Consequently, the $MAOC_{max}$ of 1:1 clay-dominated systems may rival or surpass that of their 2:1 counterparts under specific conditions (Kleber et al., 2007). While the $MAOC_{max}$ estimated based on 1:1 clay mineralogy may be underestimated (i.e., CSD is overestimated), it shows an overall trend consistent with estimates derived from 2:1 clay mineralogy. This consistency underscores the robustness of our analytical findings and indicates that they do not affect the interpretation of the underlying mechanisms influencing SOC and its fractions. Future work incorporating direct characterization of soil mineralogy into CSD models will be crucial for precisely estimating the MAOC stabilization potential at the site scale. Second, as exemplified in our study, mechanistic experiments should be synergistically integrated with large-scale surveys. For instance, controlled experiments focusing on mycorrhizal fungi are needed further to elucidate their specific effects on SOC and its fractions. The integration of approaches will deepen the mechanistic understanding of soil carbon sequestration processes in both croplands and adjacent planted forests. Third, although this study specifically examined ecological-functional planted forests, it should be recognized that other planted forest types exist (e.g., erosion-control planted forests in ecologically fragile areas). The applicability of these findings to other planted forest types necessitates further investigation.

5. Conclusions

This study elucidates the distinct mechanisms influencing SOC storage in croplands and adjacent planted forests in Eastern China. Our results reveal a fundamental divergence in both the pathways of accumulation and the drivers of stabilization between the two land-use systems. In cropland soils, SOC accumulation involved a substantial

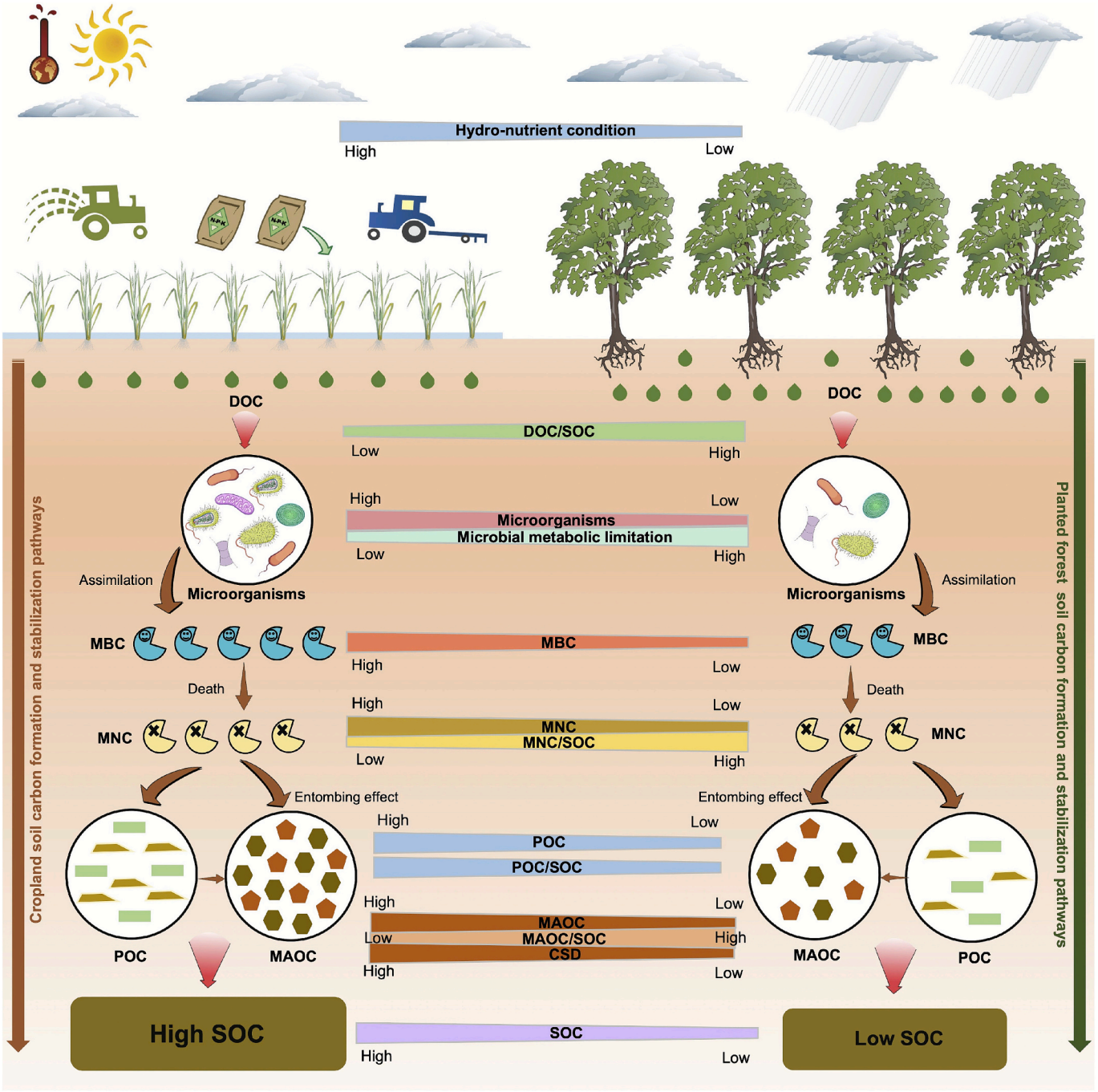

Fig. 7. Schematic diagram of the pathways of microbial-mediated DOC flowing sequentially to MBC, MNC, POC, and MAOC, and finally forming SOC in croplands and adjacent planted forests. DOC/SOC, DOC to SOC ratio; POC/SOC, POC to SOC ratio; MAOC/SOC, MAOC to SOC ratio; MNC/SOC, MNC to SOC ratio.

dual contribution from POC and MAOC, with the microbial carbon pump playing a central role in transforming DOC into persistent MNC. SOC and its fractions in croplands were primarily mediated by biotic drivers, including the integrated activity of AMF and EcMF. Conversely, in adjacent planted forests, SOC storage was dominated by MAOC and affected predominantly by abiotic factors, leading to higher overall SOC stability. Collectively, these findings demonstrate a critical trade-off between the active, biotically-driven carbon cycling (higher input, lower stability) of croplands and the abiotically-stabilized, stable carbon pools of planted forests. This study demonstrates that the conversion of croplands to planted forests can enhance SOC stability despite a potential decline in its content, offers novel insights into the mechanisms of SOC accumulation and stabilization, and provides valuable guidance for managing carbon sequestration in such land-use transitions.

CRediT authorship contribution statement

Jie Liu: Writing – review & editing, Writing – original draft, Visualization, Validation, Software, Project administration, Methodology, Investigation, Formal analysis, Data curation, Conceptualization. **Lin Yang:** Writing – review & editing, Supervision, Resources, Project administration, Funding acquisition, Conceptualization. **Jie Wang:** Writing – review & editing, Investigation. **Lei Zhang:** Writing – review & editing, Supervision. **Yongqi Qian:** Writing – review & editing, Investigation. **Ren Wei:** Writing – review & editing, Investigation. **Wenkai Cui:** Writing – review & editing, Investigation. **Chenghu Zhou:**

Writing – review & editing, Supervision, Resources.

Declaration of competing interest

The authors declare that they have no known competing financial interests or personal relationships that could have appeared to influence the work reported in this paper.

Acknowledgements

This work was supported by the National Natural Science Foundation of China (grant number 42471468) and the Fundamental Research Funds for the Central Universities (grant number 0209-14380115). Jie Liu was supported by the Postgraduate Research & Practice Innovation Program of Jiangsu Province (grant number KYCX25_0209).

Appendix A. Supplementary data

Supplementary data to this article can be found online at https://doi.org/10.1016/j.apsoil.2026.106808.

Data availability

Data will be made available on request.

References

Angst, G., Mueller, K.E., Castellano, M.J., Vogel, C., Wiesmeier, M., Mueller, C.W., 2023. Unlocking complex soil systems as carbon sinks: multi-pool management as the key. Nat. Commun. 14, 2967. https://doi.org/10.1038/s41467-023-38700-5.

Archer, E., 2023. rfPermute: estimate permutation p-values for random forest importance metrics. R package version 2.5.2. https://CRAN.R-project.org/package=rfPermute (doi:10.32614/CRAN.package.rfPermute).

Batjes, N.H., 1996. Total carbon and nitrogen in the soils of the world. Eur. J. Soil Sci. 47, 151–163. https://doi.org/10.1111/j.1365-2389.1996.tb01386.x.

Breure, T.S., De Rosa, D., Panagos, P., Cotrufo, M.F., Jones, A., Lugato, E., 2025. Revisiting the soil carbon saturation concept to inform a risk index in European agricultural soils. Nat. Commun. 16, 2538. https://doi.org/10.1038/s41467-025-57355-y.

Callahan, B.J., McMurdie, P.J., Rosen, M.J., Han, A.W., Johnson, A.J.A., Holmes, S.P., 2016. DADA2: high-resolution sample inference from Illumina amplicon data. Nat. Methods 13, 581–583. https://doi.org/10.1038/nmeth.3869.

Castellano, M.J., Mueller, K.E., Olk, D.C., Sawyer, J.E., Six, J., 2015. Integrating plant litter quality, soil organic matter stabilization, and the carbon saturation concept. Glob. Chang. Biol. 21, 3200–3209. https://doi.org/10.1111/gcb.12982.

Chen, X.B., Hu, Y.J., Xia, Y.H., Zheng, S.M., Ma, C., Rui, Y.C., He, H.B., Huang, D.Y., Zhang, Z.H., Ge, T.D., Wu, J.S., Guggenberger, G., Kuzyakov, Y., Su, Y.R., 2021. Contrasting pathways of carbon sequestration in paddy and upland soils. Glob. Chang. Biol. 27, 2478–2490. https://doi.org/10.1111/gcb.15595.

Chen, R., Yin, L.M., Wang, X.H., Chen, T.T., Jia, L.Q., Jiang, Q., Lyu, M.K., Yao, X.D., Chen, G.S., 2023. Mineral-associated organic carbon predicts the variations in microbial biomass and specific enzyme activities in a subtropical forest. Geoderma 439, 116671. https://doi.org/10.1016/j.geoderma.2023.116671.

Cheng, K., Yang, H.T., Tao, S.L., Su, Y.J., Guan, H.C., Ren, Y., Hu, T.Y., Li, W.K., Xu, G.C., Chen, M.X., Lu, X.C., Yang, Z.K., Tang, Y.H., Ma, K.P., Fang, J.Y., Guo, Q.H., 2024. Carbon storage through China's planted forest expansion. Nat. Commun. 15, 4106. https://doi.org/10.1038/s41467-024-48546-0.

Cotrufo, M.F., Lavallee, J.M., 2022. Soil organic matter formation, persistence, and functioning: a synthesis of current understanding to inform its conservation and regeneration. Adv. Agron. 172, 1–66. https://doi.org/10.1016/bs.agron.2021.11.002.

Cotrufo, M.F., Wallenstein, M.D., Boot, C.M., Denef, K., Paul, E., 2013. The Microbial Efficiency-Matrix Stabilization (MEMS) framework integrates plant litter decomposition with soil organic matter stabilization: do labile plant inputs form stable soil organic matter? Glob. Chang. Biol. 19, 988–995. https://doi.org/10.1111/gcb.12113.

Cotrufo, M.F., Ranalli, M.G., Haddix, M.L., Six, J., Lugato, E., 2019. Soil carbon storage informed by particulate and mineral-associated organic matter. Nat. Geosci. 12, 989–994. https://doi.org/10.1038/s41561-019-0484-6.

Cotrufo, M.F., Haddix, M.L., Kroeger, M.E., Stewart, C.E., 2022. The role of plant input physical-chemical properties, and microbial and soil chemical diversity on the formation of particulate and mineral-associated organic matter. Soil Biol. Biochem. 168, 108648. https://doi.org/10.1016/j.soilbio.2022.108648.

Craig, M.E., Mayes, M.A., Sulman, B.N., Walker, A.P., 2021. Biological mechanisms may contribute to soil carbon saturation patterns. Glob. Chang. Biol. 27, 2633–2644. https://doi.org/10.1111/gcb.15584.

Crowther, T.W., Van den Hoogen, J., Wan, J., Mayes, M.A., Keiser, A., Mo, L., Averill, C., Maynard, D.S., 2019. The global soil community and its influence on biogeochemistry. Science 365, eaav0550. https://doi.org/10.1126/science.aav0550.

de Goede, S.P., Hannula, S.E., Jansen, B., Morriën, E., 2025. Fungal-mediated soil aggregation as a mechanism for carbon stabilization. ISME J. 19, wraf074. https://doi.org/10.1093/ismejo/wraf074.

Delgado-Baquerizo, M., Reich, P.B., Trivedi, C., Eldridge, D.J., Abades, S., Alfaro, F.D., Bastida, F., Berhe, A.A., Cutler, N.A., Gallardo, A., 2020. Multiple elements of soil biodiversity drive ecosystem functions across biomes. Nat. Ecol. Evol. 4, 210–220. https://doi.org/10.1038/s41559-019-1084-y.

Denef, K., Zotarelli, L., Boddey, R.M., Six, J.W., 2007. Microaggregate-associated carbon as a diagnostic fraction for management-induced changes in soil organic carbon in two Oxisols. Soil Biol. Biochem. 39, 1165–1172. https://doi.org/10.1016/j.soilbio.2006.12.024.

Deng, J., Frolking, S., Bajgain, R., Cornell, C.R., Wagle, P., Xiao, X.M., Zhou, J.Z., Basara, J., Steiner, J., Li, C.S., 2021. Improving a biogeochemical model to simulate microbial-mediated carbon dynamics in agricultural ecosystems. J. Adv. Model. Earth Syst. 13, e2021MS002752. https://doi.org/10.1029/2021MS002752.

Derrien, D., Barré, P., Basile-Doelsch, I., Cécillon, L., Chabbi, A., Crème, A., Fontaine, S., Henneron, L., Janot, N., Lashermes, G., 2023. Current controversies on mechanisms controlling soil carbon storage: implications for interactions with practitioners and policy-makers. A review. Agron. Sustain. Dev. 43, 21. https://doi.org/10.1007/s13593-023-00876-x.

Dor, M., Fan, L.C., Zamanian, K., Kravchenko, A.N., 2025. Long-term land use conversion influence on soil pore structure and organic carbon. Agric. Ecosyst. Environ. 387, 109633. https://doi.org/10.1016/j.agee.2025.109633.

Gao, Y., Huang, D.D., Zhang, Y., McLaughlin, N., Zhang, Y., Wang, Y., Chen, X.W., Zhang, S.X., Lu, Y.F., Liang, A.Z., 2024. Precipitation increment reinforced warming-induced increases in soil mineral-associated and particulate organic matter under agricultural ecosystem. Appl. Soil Ecol. 196, 105301. https://doi.org/10.1016/j.apsoil.2024.105301.

Georgiou, K., Jackson, R.B., Vindušková, O., Abramoff, R.Z., Ahlström, A., Feng, W., Harden, J.W., Pellegrini, A.F.A., Wayne Polley, H., Soong, J.L., Riley, W.J., Torn, M.S., 2022. Global stocks and capacity of mineral-associated soil organic carbon. Nat. Commun. 13, 3797. https://doi.org/10.1038/s41467-022-31540-9.

Gong, S.S., Liu, S., Li, F.F., Xu, G.X., Chen, J., Jia, L., Shi, Z.M., 2025. Natural forests vs. plantations: a meta-analysis of consequences for soil organic carbon functional fractions. J. Environ. Manag. 377, 124673. https://doi.org/10.1016/j.jenvman.2025.124673.

Haddix, M.L., Gregorich, E.G., Helgason, B.L., Janzen, H., Ellert, B.H., Cotrufo, M.F., 2020. Climate, carbon content, and soil texture control the independent formation and persistence of particulate and mineral-associated organic matter in soil. Geoderma 363, 114160. https://doi.org/10.1016/j.geoderma.2019.114160.

He, Y., Wen, Y., Li, K., Ye, S., Zhang, H., He, F., Fan, R., Wu, H., 2025. Responses of soil multifunctionality, microbial diversity, and network complexity to tree species mixing in Eucalyptus plantations. Ind. Crop. Prod. 225, 120575. https://doi.org/10.1016/j.indcrop.2025.120575.

Heckman, K., Hicks Pries, C.E., Lawrence, C.R., Rasmussen, C., Crow, S.E., Hoyt, A.M., von Fromm, S.F., Shi, Z., Stoner, S., McGrath, C., 2022. Beyond bulk: density fractions explain heterogeneity in global soil carbon abundance and persistence. Glob. Chang. Biol. 28, 1178–1196. https://doi.org/10.1111/gcb.16023.

Hu, H., Qian, C., Xue, K., Jörgensen, R.G., Keiluweit, M., Liang, C., Zhu, X., Chen, J., Sun, Y., Ni, H., 2024. Reducing the uncertainty in estimating soil microbial-derived carbon storage. Proc. Natl. Acad. Sci. USA 121, e2401916121. https://doi.org/10.1073/pnas.2401916121.

Huang, Q., Wang, B.R., Shen, J.K., Xu, F.J., Li, N., Jia, P.H., Jia, Y.J., An, S.S., Amoah, I.D., Huang, Y.M., 2024. Shifts in C-degradation genes and microbial metabolic activity with vegetation types affected the surface soil organic carbon pool. Soil Biol. Biochem. 192, 109371. https://doi.org/10.1016/j.soilbio.2024.109371.

Kaiser, K., Guggenberger, G., 2003. Mineral surfaces and soil organic matter. Eur. J. Soil Sci. 54, 219–236. https://doi.org/10.1046/j.1365-2389.2003.00544.x.

Kallenbach, C.M., Frey, S.D., Grandy, A.S., 2016. Direct evidence for microbial-derived soil organic matter formation and its ecophysiological controls. Nat. Commun. 7, 13630. https://doi.org/10.1038/ncomms13630.

Kan, Z.R., Li, Z., Amelung, W., Zhang, H.L., Lal, R., Bol, R., Bian, X., Liu, J., Xue, Y., Li, F., Yang, H., 2025. Soil carbon accrual and crop production enhanced by sustainable subsoil management. Nat. Geosci. 18, 631–638. https://doi.org/10.1038/s41561-025-01720-5.

King, A.E., Sokol, N.W., 2025. Soil carbon formation is promoted by saturation deficit and existing mineral-associated carbon, not by microbial carbon-use efficiency. Sci. Adv. 11, eadv9482. https://doi.org/10.1126/sciadv.adv9482.

Kleber, M., Sollins, P., Sutton, R., 2007. A conceptual model of organo-mineral interactions in soils: self-assembly of organic molecular fragments into zonal structures on mineral surfaces. Biogeochemistry 85, 9–24. https://doi.org/10.1007/s10533-007-9103-5.

Kleber, M., Bourg, I.C., Coward, E.K., Hansel, C.M., Myneni, S.C., Nunan, N., 2021. Dynamic interactions at the mineral–organic matter interface. Nat. Rev. Earth Environ. 2, 402–421. https://doi.org/10.1038/s43017-021-00162-y.

Langille, M.G., Zaneveld, J., Caporaso, J.G., McDonald, D., Knights, D., Reyes, J.A., Clemente, J.C., Burkepile, D.E., Vega Thurber, R.L., Knight, R., 2013. Predictive functional profiling of microbial communities using 16S rRNA marker gene sequences. Nat. Biotechnol. 31, 814–821. https://doi.org/10.1038/nbt.2676.

Lavallee, J.M., Soong, J.L., Cotrufo, M.F., 2020. Conceptualizing soil organic matter into particulate and mineral-associated forms to address global change in the 21st century. Glob. Chang. Biol. 26, 261–273. https://doi.org/10.1111/gcb.14859.

Lefcheck, J.S., 2016. piecewiseSEM: piecewise structural equation modelling in r for ecology, evolution, and systematics. Methods Ecol. Evol. 7, 573–579. https://doi.org/10.1111/2041-210X.12512.
Lehmann, J., Kleber, M., 2015. The contentious nature of soil organic matter. Nature 528, 60–68. https://doi.org/10.1038/nature16069.
Li, Y.T., Xie, X.N., Zhu, Z.J., Liu, K., Liu, W.X., Wang, J., 2022. Land use driven change in soil organic carbon affects soil microbial community assembly in the riparian of Three Gorges Reservoir Region. Appl. Soil Ecol. 176, 104467. https://doi.org/10.1016/j.apsoil.2022.104467.
Li, Z., Duan, X., Guo, X.B., Gao, W., Li, Y., Zhou, P., Zhu, Q.H., O'Donnell, A.G., Dai, K., Wu, J.S., 2024. Microbial metabolic capacity regulates the accrual of mineral-associated organic carbon in subtropical paddy soils. Soil Biol. Biochem. 195, 109457. https://doi.org/10.1016/j.soilbio.2024.109457.
Li, T., Phillips, R.P., Rillig, M.C., Angst, G., Kiers, E.T., Bonfante, P., Eisenhauer, N., Liu, Z., 2025a. Mycorrhizal allies: synergizing forest carbon and multifunctional restoration. Trends Ecol. Evol. 40, 983–994. https://doi.org/10.1016/j.tree.2025.07.004.
Li, Y.L., Wei, X.Q., Yan, J., Du, Z.L., Lv, Y.Z., Zhou, H., 2025b. Divergent stabilization characteristics of soil organic carbon between topsoil and subsoil under different land use types. Catena 252, 108838. https://doi.org/10.1016/j.catena.2025.108838.
Liaw, A., Wiener, M., 2002. Classification and regression by randomForest. R News 2 (3), 18–22. https://CRAN.R-project.org/doc/Rnews/.
Liu, S., García-Palacios, P., Tedersoo, L., Guirado, E., van der Heijden, M.G., Wagg, C., Chen, D., Wang, Q., Wang, J., Singh, B.K., 2022. Phylotype diversity within soil fungal functional groups drives ecosystem stability. Nat. Ecol. Evol. 6, 900–909. https://doi.org/10.1038/s41559-022-01756-5.
Liu, D., Zhou, Z., Iqbal, S., Dou, T.T., Bonito, G., Liu, W., An, S., Chater, C., Pérez-Moreno, J., Che, R., Jones, D.L., Yu, F., 2024. Fungal necromass contribution to carbon sequestration in global croplands: a meta-analysis of driving factors and conservation practices. Sci. Total Environ. 949, 174954. https://doi.org/10.1016/j.scitotenv.2024.174954.
Liu, J., Yang, L., Adams, J.M., Zhang, L., Wang, J., Wei, R., Zhou, C.H., 2025a. Divergent biotic-abiotic mechanisms of soil organic carbon storage between bulk and rhizosphere soils of rice paddies in the Yangtze River Delta. J. Environ. Manage 389, 126179. https://doi.org/10.1016/j.jenvman.2025.126179.
Liu, M.L., Zheng, S.L., Pendall, E., Smith, P., Liu, J.J., Li, J.Q., Fang, C.M., Li, B., Nie, M., 2025b. Unprotected carbon dominates decadal soil carbon increase. Nat. Commun. 16, 2008. https://doi.org/10.1038/s41467-025-57354-z.
López-Mondéjar, R., Brabcová, V., Štursová, M., Davidová, A., Jansa, J., Cajthaml, T., Baldrian, P., 2018. Decomposer food web in a deciduous forest shows high share of generalist microorganisms and importance of microbial biomass recycling. ISME J. 12, 1768–1778. https://doi.org/10.1038/s41396-018-0084-2.
Luo, Z.K., Feng, W.T., Luo, Y.Q., Baldock, J., Wang, E.L., 2017. Soil organic carbon dynamics jointly controlled by climate, carbon inputs, soil properties and soil carbon fractions. Glob. Chang. Biol. 23, 4430–4439. https://doi.org/10.1111/gcb.13767.
Magill, A.H., Aber, J.D., 2000. Dissolved organic carbon and nitrogen relationships in forest litter as affected by nitrogen deposition. Soil Biol. Biochem. 32, 603–613. https://doi.org/10.1016/S0038-0717(99)00187-X.
Mao, C., Kou, D., Chen, L.Y., Qin, S.Q., Zhang, D.Y., Peng, Y.F., Yang, Y.H., 2020. Permafrost nitrogen status and its determinants on the Tibetan Plateau. Glob. Chang. Biol. 26, 5290–5302. https://doi.org/10.1111/gcb.15205.
Marriott, E.E., Wander, M.M., 2006. Total and labile soil organic matter in organic and conventional farming systems. Soil Sci. Soc. Am. J. 70, 950–959. https://doi.org/10.2136/sssaj2005.0241.
Marschner, B., Bredow, A., 2002. Temperature effects on release and ecologically relevant properties of dissolved organic carbon in sterilised and biologically active soil samples. Soil Biol. Biochem. 34, 459–466. https://doi.org/10.1016/S0038-0717(01)00203-6.
Mebius, L.J., 1960. A rapid method for the determination of organic carbon in soil. Anal. Chim. Acta 22, 120–124. https://doi.org/10.1016/S0003-2670(00)88254-9.
Mi, W., Dong, H., Chen, H., Gao, F., Zhu, K., Hong, Y., Fan, J., Wu, Q., Yan, P., Chen, S., 2025. Diverse protective mechanisms drive changes in functional carbon pools of paddy soil under continuous biochar and inorganic fertilizer application. Appl. Soil Ecol. 213, 106305. https://doi.org/10.1016/j.apsoil.2025.10630.
Michalzik, B., Kalbitz, K., Park, J.-H., Solinger, S., Matzner, E., 2001. Fluxes and concentrations of dissolved organic carbon and nitrogen-a synthesis for temperate forests. Biogeochemistry 52, 173–205. https://doi.org/10.1023/A:1006441620810.
Minasny, B., McBratney, A.B., 2006. A conditioned Latin hypercube method for sampling in the presence of ancillary information. Comput. Geosci. 32, 1378–1388. https://doi.org/10.1016/j.cageo.2005.12.009.
Niu, Y.L., Li, Y., Lou, M.X., Cheng, Z., Ma, R.J., Guo, H., Zhou, J., Jia, H.T., Fan, L.C., Wang, T.C., 2024. Microbial transformation mechanisms of particulate organic carbon to mineral-associated organic carbon at the chemical molecular level: highlighting the effects of ambient temperature and soil moisture. Soil Biol. Biochem. 195, 109454. https://doi.org/10.1016/j.soilbio.2024.109454.
O'brien, R.M., 2007. A caution regarding rules of thumb for variance inflation factors. Qual. Quant. 41, 673–690. https://doi.org/10.1007/s11135-006-9018-6.
Pölme, S., Abarenkov, K., Henrik Nilsson, R., 2020. FungalTraits: a user-friendly traits database of fungi and fungus-like stramenopiles. Fungal Divers. 105, 1–16. https://doi.org/10.1007/s13225-020-00466-2.
R Core Team, 2025. R: a language and environment for statistical computing, R Foundation for Statistical Computing, Vienna, Austria. https://www.R-project.org/ (accessed 2025-04-11).
Raffa, D.W., Ros, M., Testani, E., Carrascosa-Robles, Á., Ciaccia, C., De Toma, A., Fontaine, S., Piton, G., Suproniene, S., Kadziene, G., Šlepetiene, A., Sail, S., Sanchez-Moreno, S., Un, A., Peixoto, L., Trinchera, A., 2025. Linking plant and microbial traits to soil organic carbon dynamics: a functional approach. Appl. Soil Ecol. 213, 106308. https://doi.org/10.1016/j.apsoil.2025.106308.
Si, Q.T.N., Chen, K.L., Wei, B., Zhang, Y.W., Sun, X., Liang, J.Y., 2024. Dissolved carbon flow to particulate organic carbon enhances soil carbon sequestration. Soil 10, 441–450. https://doi.org/10.5194/soil-10-441-2024.
Six, J., Conant, R.T., Paul, E.A., Paustian, K., 2002. Stabilization mechanisms of soil organic matter: implications for C-saturation of soils. Plant Soil 241, 155–176. https://doi.org/10.1023/A:1016125726789.
Soinne, H., Hyyrynen, M., Jokubė, M., Keskinen, R., Hyväluoma, J., Pihlainen, S., Hyytiäinen, K., Miettinen, A., Rasa, K., Lemola, R., 2024. High organic carbon content constricts the potential for stable organic carbon accrual in mineral agricultural soils in Finland. J. Environ. Manag. 352, 119945. https://doi.org/10.1016/j.jenvman.2023.119945.
Sokol, N.W., Bradford, M.A., 2019. Microbial formation of stable soil carbon is more efficient from belowground than aboveground input. Nat. Geosci. 12, 46–53. https://doi.org/10.1038/s41561-018-0258-6.
Sokol, N.W., Whalen, E.D., Jilling, A., Kallenbach, C., Pett-Ridge, J., Georgiou, K., 2022. Global distribution, formation and fate of mineral-associated soil organic matter under a changing climate: a trait-based perspective. Funct. Ecol. 36, 1411–1429. https://doi.org/10.1111/1365-2435.14040.
Song, X., Wu, H., Li, S., He, P., Wu, X., 2025. The need to update and refine concepts relating to mineral-associated organic matter saturation in soil. Soil Biol. Biochem. 202, 109672. https://doi.org/10.1016/j.soilbio.2024.109672.
Sun, H., Wang, L.L., Kumar, A., Auwal, M., Van Zwieten, L., Ge, T.D., Fu, Y.Y., Kuzyakov, Y., 2025. Nutrient availability mediates organic carbon turnover in paddy soils through regulating microbial metabolism. Geoderma 458, 117313. https://doi.org/10.1016/j.geoderma.2025.117313.
Tang, B., Rocci, K.S., Lehmann, A., Rillig, M.C., 2023. Nitrogen increases soil organic carbon accrual and alters its functionality. Glob. Chang. Biol. 29, 1971–1983. https://doi.org/10.1111/gcb.16588.
Tian, J., Dungait, J.A., Hou, R., Deng, Y., Hartley, I.P., Yang, Y., Kuzyakov, Y., Zhang, F., Cotrufo, M.F., Zhou, J., 2024. Microbially mediated mechanisms underlie soil carbon accrual by conservation agriculture under decade-long warming. Nat. Commun. 15, 377. https://doi.org/10.1038/s41467-023-44647-4.
von Lützow, M., Kögel-Knabner, I., Ekschmitt, K., Flessa, H., Guggenberger, G., Matzner, E., Marschner, B., 2007. SOM fractionation methods: relevance to functional pools and to stabilization mechanisms. Soil Biol. Biochem. 39, 2183–2207. https://doi.org/10.1016/j.soilbio.2007.03.007.
Wang, B.R., An, S.S., Liang, C., Liu, Y., Kuzyakov, Y., 2021. Microbial necromass as the source of soil organic carbon in global ecosystems. Soil Biol. Biochem. 162, 108422. https://doi.org/10.1016/j.soilbio.2021.108422.
Wang, C., Wang, X., Zhang, Y., Morrissey, E., Liu, Y., Sun, L.F., Qu, L.R., Sang, C.P., Zhang, H., Li, G.C., Zhang, L.L., Fang, Y.T., 2023. Integrating microbial community properties, biomass and necromass to predict cropland soil organic carbon. ISME Commun. 3, 86. https://doi.org/10.1038/s43705-023-00300-1.
Wang, X.X., Zhang, H.R., Cao, D., Wu, C.Y., Wang, X.T., Wei, L., Guo, B., Wang, S., Ding, J.N., Chen, H., Chen, J.P., Ge, T.D., Zhu, Z.K., 2024a. Microbial carbon and phosphorus metabolism regulated by C:N:P stoichiometry stimulates organic carbon accumulation in agricultural soils. Soil Tillage Res. 242, 106152. https://doi.org/10.1016/j.still.2024.106152.
Wang, X.X., Zhou, L.Y., Fu, Y.L., Jiang, Z., Jia, S.X., Song, B.Q., Liu, D.Q., Zhou, X.H., 2024b. Drought-induced changes in rare microbial community promoted contribution of microbial necromass C to SOC in a subtropical forest. Soil Biol. Biochem. 189, 109252. https://doi.org/10.1016/j.soilbio.2023.109252.
Wang, W., Li, G.X., Li, J.W., Lin, Y.X.F., Bian, H.F., Wang, Y., He, C.G., 2025a. Dissolved organic matter drives soil carbon mineralization efficiency and indirectly affects stocks after converting forest swamps to cropland. Land Degrad. Dev. https://doi.org/10.1002/ldr.70183.
Wang, Y., Gunina, A., Yang, D.F., Sun, T., Kuzyakov, Y., 2025b. Carbon pathways in soil: unraveled by ^{13}C natural abundance. Soil Biol. Biochem., 109872 https://doi.org/10.1016/j.soilbio.2025.109872.
Wei, L., Ge, T.D., Zhu, Z.K., Luo, Y., Yang, Y.H., Xiao, M.L., Yan, Z.F., Li, Y.H., Wu, J.S., Kuzyakov, Y., 2021. Comparing carbon and nitrogen stocks in paddy and upland soils: accumulation, stabilization mechanisms, and environmental drivers. Geoderma 398, 115121. https://doi.org/10.1016/j.geoderma.2021.115121.
Wilson, G.W., Rice, C.W., Rillig, M.C., Springer, A., Hartnett, D.C., 2009. Soil aggregation and carbon sequestration are tightly correlated with the abundance of arbuscular mycorrhizal fungi: results from long-term field experiments. Ecol. Lett. 12, 452–461. https://doi.org/10.1111/j.1461-0248.2009.01303.x.
Witzgall, K., Vidal, A., Schubert, D.I., Höschen, C., Schweizer, S.A., Buegger, F., Pouteau, V., Chenu, C., Mueller, C.W., 2021. Particulate organic matter as a functional soil component for persistent soil organic carbon. Nat. Commun. 12, 4115. https://doi.org/10.1038/s41467-021-24192-8.
Wu, J., Joergensen, R.G., Pommerening, B., Chaussod, R., Brookes, P.C., 1990. Measurement of soil microbial biomass C by fumigation-extraction—an automated procedure. Soil Biol. Biochem. 22, 1167–1169. https://doi.org/10.1016/0038-0717(90)90046-3.
Wu, D., Wu, L., Liu, K.L., Shang, J.Y., Zhang, W.J., 2024. Contrasting effects of iron oxides on soil organic carbon accumulation in paddy and upland fields under long-term fertilization. J. Environ. Manag. 369, 122286. https://doi.org/10.1016/j.jenvman.2024.122286.
Xiao, L.M., Zhang, W., Hu, P.L., Vesterdal, L., Zhao, J., Tang, L., Xiao, D., Wang, K.L., 2023. Mosses stimulate soil carbon and nitrogen accumulation during vegetation restoration in a humid subtropical area. Soil Biol. Biochem. 184, 109127. https://doi.org/10.1016/j.soilbio.2023.109127.

Xu, X.F., Thornton, P.E., Post, W.M., 2013. A global analysis of soil microbial biomass carbon, nitrogen and phosphorus in terrestrial ecosystems. Glob. Ecol. Biogeogr. 22, 737–749. https://doi.org/10.1111/geb.1202.

Yang, Y., Gunina, A., Cheng, H., Liu, L.X., Wang, B.R., Dou, Y.X., Wang, Y.Q., Liang, C., An, S.S., Chang, S.X., 2025. Unlocking mechanisms for soil organic matter accumulation: carbon use efficiency and microbial necromass as the keys. Glob. Chang. Biol. 31, e70033. https://doi.org/10.1111/gcb.70033.

Zhang, X.D., Amelung, W., 1996. Gas chromatographic determination of muramic acid, glucosamine, mannosamine, and galactosamine in soils. Soil Biol. Biochem. 28, 1201–1206. https://doi.org/10.1016/0038-0717(96)00117-4.

Zhang, X.Y., Jia, J., Chen, L.T., Chu, H.Y., He, J.S., Zhang, Y.J., Feng, X.J., 2021. Aridity and NPP constrain contribution of microbial necromass to soil organic carbon in the QinghaiTibet alpine grasslands. Soil Biol. Biochem. 156, 108213. https://doi.org/10.1016/j.soilbio.2021.108213.

Zhang, M.L., Che, R.X., Cheng, Z.B., Zhao, H.K., Wu, C.W., Hu, J.M., Zhang, S., Liu, D., Cui, X.Y., Wu, Y.B., 2023. Decades of reforestation significantly change microbial necromass, glomalin, and their contributions to soil organic carbon. Agric. Ecosyst. Environ. 346, 108362. https://doi.org/10.1016/j.agee.2023.108362.

Zhang, Z.R., Gao, H., Gao, X.X., Huang, S.R., Niu, S.L., Lugato, E., Xia, X.H., 2025. Short-term warming supports mineral-associated carbon accrual in abandoned croplands. Nat. Commun. 16, 344. https://doi.org/10.1038/s41467-024-55765-y.

Zhao, Q., Bell, S., Kukkadapu, R., Richardson, J., Cliff, J., Bowden, M., Leichty, S., Hofmockel, K.S., 2025a. Accumulation of soil microbial necromass controlled by microbe-mineral interactions. Environ. Sci. Technol. 59, 17558–17570. https://doi.org/10.1021/acs.est.5c01482.

Zhao, Y., Biswas, A., Liu, M., Han, X., Lu, X., Chen, X., Hao, X., Zou, W., 2025b. Land use effects on soil carbon retention through glomalin-mediated aggregation. Geoderma 456, 117252. https://doi.org/10.1016/j.geoderma.2025.117252.

Zhou, Z.H., Ren, C.J., Wang, C.K., Delgado-Baquerizo, M., Luo, Y.Q., Luo, Z.K., Du, Z.G., Zhu, B., Yang, Y.H., Jiao, S., Zhao, F.Z., Cai, A.D., Yang, G.H., Wei, G.H., 2024. Global turnover of soil mineral-associated and particulate organic carbon. Nat. Commun. 15, 5329. https://doi.org/10.1038/s41467-024-49743-7.

Zhou, G., Li, G., Liang, H., Liu, R., Ma, Z., Gao, S., Chang, D., Liu, J., Chadwick, D.R., Jones, D.L., Cao, W., 2025. Green manure coupled with straw returning increases soil organic carbon via decreased priming effect and enhanced microbial carbon pump. Glob. Chang. Biol. 31, e70232. https://doi.org/10.1111/gcb.70232.